NASA CR-112273

EXPERIMENTAL PROGRAM TO DETERMINE LONG-TERM CHARACTERISTICS OF THE MDE PRESSURE TRANSDUCERS

Final Report

January 1973

Prepared under Contract No. NAS1-10175 by
RESEARCH TRIANGLE INSTITUTE
Research Triangle Park, N. C.

for Langley Research Center

NATIONAL AERONATUICS AND SPACE ADMINISTRATION

FOREWORD

This report describes investigation by the Research Triangle Institute, Research Triangle Park, N. C., on NASA Contract NAS1-10175, "Experimental Program to Determine Long-Term Characteristics of Pressure Transducers." These investigations were monitored by Mr. L. R. McMaster of the Instrument Research Division, Langley Research Center.

Numerous Langley Research Center personnel contributed significantly to these investigations. In addition to Mr. McMaster, Messrs. W. H. Kinard, R. L. O'Neal, J. M. Alvarez and John Thompson participated in these investigations. Mr. P. C. Kassel of Langley Research Center assisted Dr. L. K. Monteith of N. C. State University, a consultant to RTI, in completing the SREL facility experiments described in Appendices B and C of this report.

These investigations were performed in the Instrumentation, Measurements and Device Research Department of the Research Triangle Institute, Mr. J. B. Tommerdahl, Manager. Mr. Tommerdahl was Laboratory Supervisor and C. D. Parker was Project Leader. Other Institute personnel who contributed significantly to these investigations include Dr. J. J. Wortman, S. R. Stilley, C. E. Moore and P. P. Rasberry.

ABSTRACT

The pressure-cell sensors developed for the Pioneer 10/G Meteoroid Detection Experiments (MDE) were further investigated to enhance their application on Pioneer 10 and Pioneer G and their potential as a sensor in other MDE applications. Their Paschen characteristics were further investigated, and the effects of variations in geometry, Ni^{63} platings (for initial ionizations) and sealing pressures were determined. The effects of extensive pre-flight testing and proton and heavy ion space radiation were investigated. Finally, flight-quality pressure panels/cells were committed to long-term testing to demonstrate their suitability for the Pioneer 10/G Missions.

TABLE OF CONTENTS

LIST OF TABLES (continued)

LIST OF ILLUSTRATIONS

LIST OF ILLUSTRATIONS (continued)

LIST OF TABLES

EXPERIMENTAL PROGRAM TO DETERMINE LONG-TERM CHARACTERISTICS OF THE MDE PRESSURE TRANSDUCER

By C. D. Parker
Research Triangle Institute

SECTION I

INTRODUCTION

This report describes the investigations under National Aeronautics and Space Administration (NASA) Contract No. NAS1-10175, "Experimental Program to Determine Long-Term Characteristics of Pressure Transducers." These investigations have been in direct support of the Meteoroid Detection Experiment (MDE) for Pioneer 10/G, and expand upon work completed under a preceding contract, NAS1-9420, "Evaluation of a Gas Discharge Transducer and Associated Instrumentation Necessary for the Asteroid Belt Meteoroid Experiment." An earlier report describes this preceding work, and familiarity with those investigations is assumed in the preparation of this report [Ref. 1].

Pioneer 10 was launched on March 2, 1972 and Pioneer G is scheduled for launch from Cape Kennedy in April of 1973. These spacecrafts will carry the MDE Experiment through the one-hundred-fifty-million mile wide Asteroid Belt and approach the vicinity of the planet Jupiter. The MDE Experiment will provide a measure of the spatial density of micrometeoroids in the 10^{-9} g mass range between Earth and Jupiter and especially in the Asteroid Belt. These experiments consist of a group of pressurized cells exposed so as to impact with meteoroids during the Pioneer 10/G flights and associated instrumentation to provide a readout of the number of cells penetrated by impact with meteoroids.

At the beginning of the current contract, the MDE experiment design had evolved to approximately its current configuration. The pressure panel configuration and fabrication procedures were well defined, a suitable pressurizing gas had been identified, an initial ionization source was specified and the pressure cells characterized so as to provide for interfacing with the electronics. Prototype panels were being fabricated for additional testing in preparation for flight hardware fabrication. The electronic system design was completed and much of the flight hardware fabricated.

The primary objective of the program reported herein was to conduct long-term life tests on flight-type pressure panels. These test results are discussed in this report. Additionally, numerous other tests were conducted which were concluded to have potential for enhancing the Pioneer 10, Pioneer G or future MDE experiments. These results, too, are included in this report. Studies completed during these investigations include studies of the effects of Ni^{63} variations and especially of using significantly less quantities of Ni^{63}, studies relating to variations in electrode geometry, the effects of ambient pressure on the firing characteristics of sealed pressure cells, and studies relating to the effects of the external, space radiation environment on the pressure cell characteristics. The principal activity, of course, was the long-term characterization studies under simulated space conditions.

Description of the MDE Experiment

The Pioneer MDE Experiment has been previously described [Ref. 1]. In the interest of completeness, a brief description is included herein.

The MDE Experiment consists of a number of pressurized cells exposed to the meteoroid environment during the Pioneer 10/G flights. Each of these sealed cells has associated circuitry that provides a count of the number of cells penetrated by meteoroids. Figure 1 is a simplified block diagram of the experiment. The pressurized cells are located in thirteen (13) pressure panels mounted on the back of the Pioneer spacecraft antenna, and each panel is compartmented into eighteen (18) individual cells. The pressure cells are instrumented with a pair of electrodes (a transducer) which causes each cell to function as a cold cathode discharge tube, and the Paschen characteristics of the tube are exploited in a cell-leak detection scheme. The transducer circuitry supplies the required high voltage to the transducers, provides a suitable signal to the counters when a transducer fires and limits power consumed by a firing transducer. The time control counter functions to advance the event counter by only one count whenever a transducer fires and provides time for the cell to leak to a vacuum before counting additional firings. The event counter is a recycling counter that is serially read-out to the spacecraft by the multiplexer upon receipt of word-gate and bit-rate commands. The power converter receives 28 Vdc from the spacecraft and supplies the voltages required by the experiment. The power converter can be turned ON and OFF on command from the spacecraft. Design details of the MDE Experiment largely reflect limitations on power, weight and size imposed by the Pioneer spacecraft capability [Ref. 2].

The MDE pressure cells are fabricated by placing a 1 mil sheet of stainless steel over a 2 mil sheet and seam-welding the two to form the 18 individual cells. Figure 2 is a photograph of a completed pressure

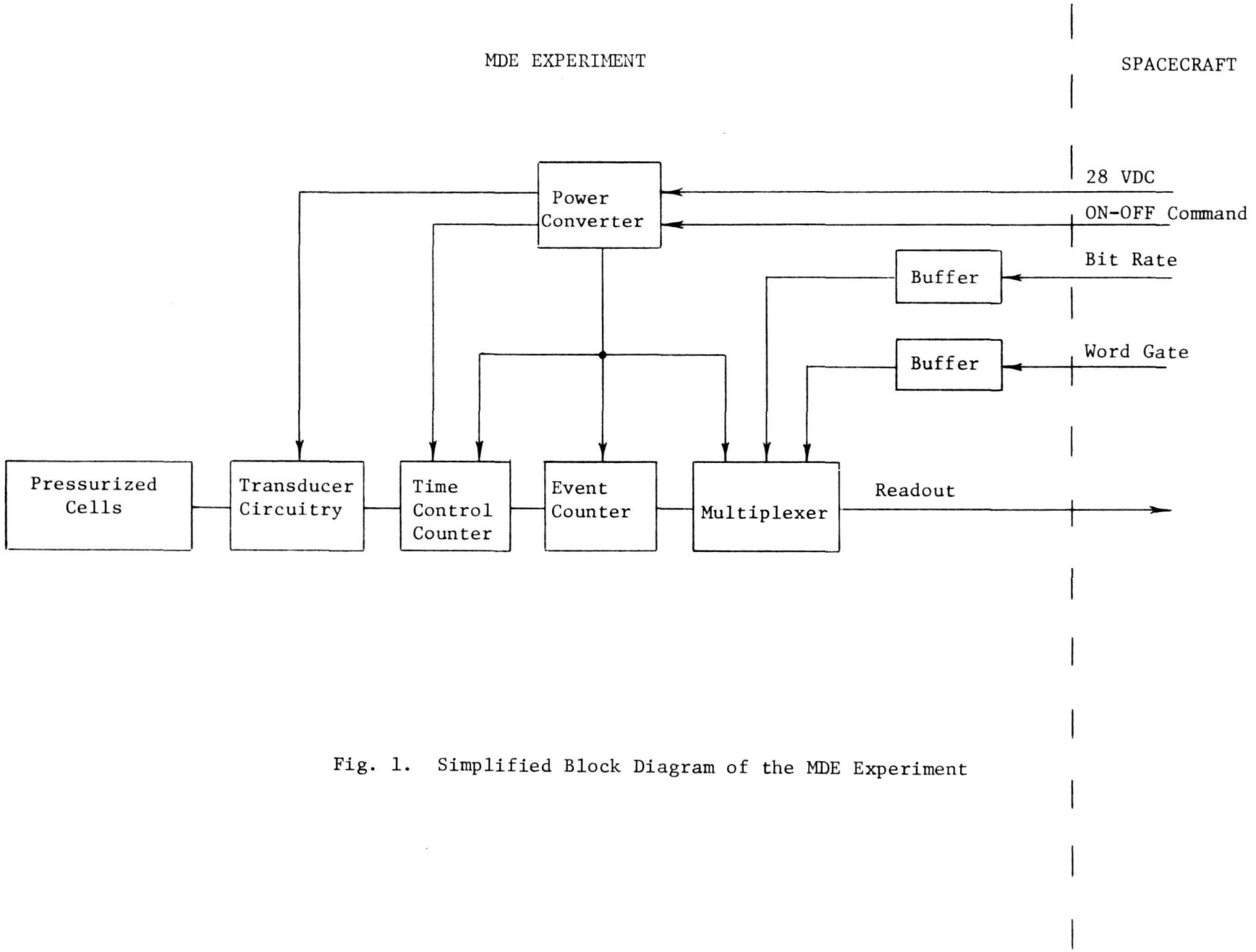

Fig. 1. Simplified Block Diagram of the MDE Experiment

NASA
L-70-5456

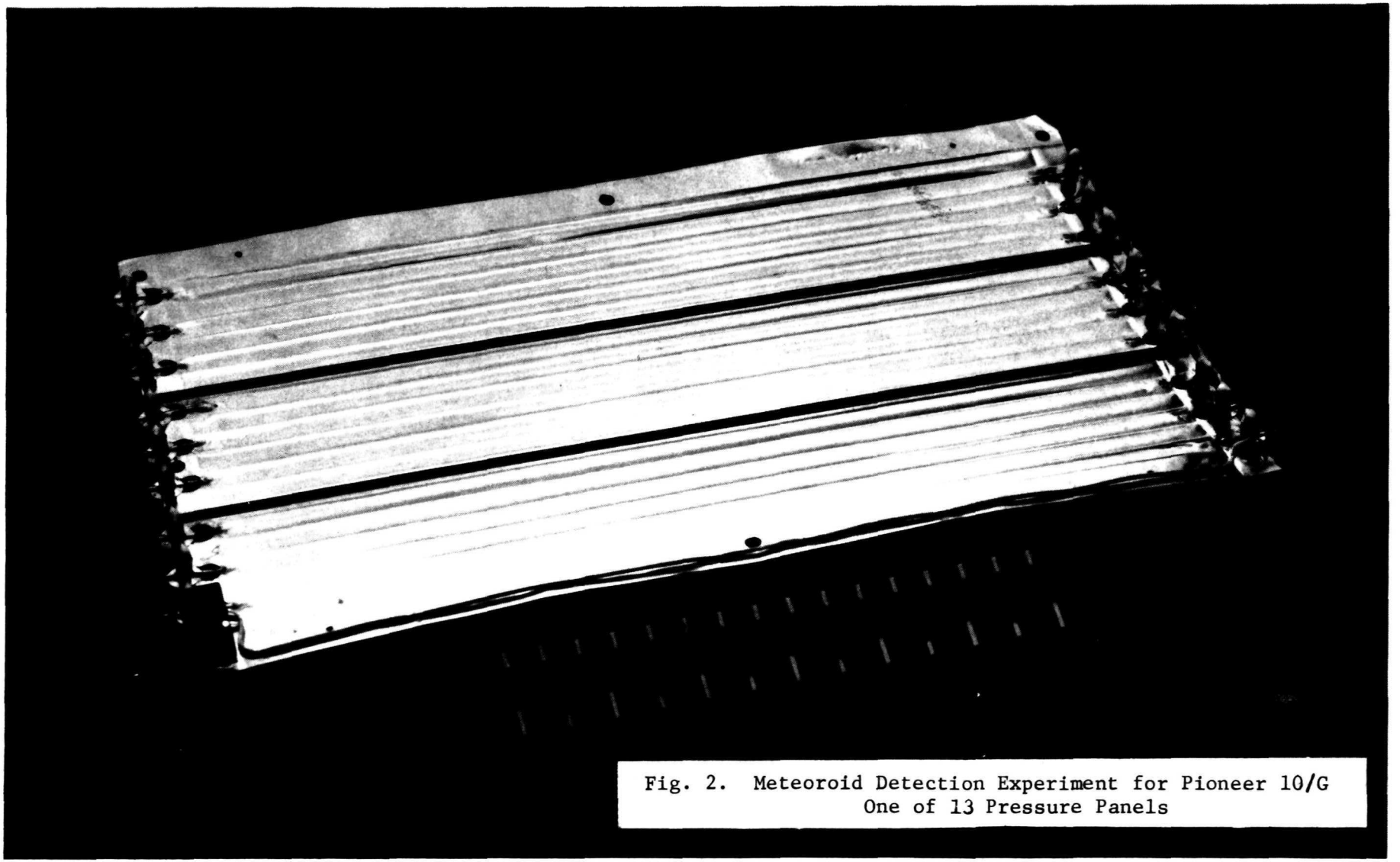

Fig. 2. Meteoroid Detection Experiment for Pioneer 10/G
One of 13 Pressure Panels

panel showing the 18 cells with transducers and wiring in place. Adjacent cells have transducer attachments at opposite ends to provide space for wiring, and two folds are symmetrically located on the panel for expansion and stress relief. Each cell is instrumented with a pair of tin-plated kovar electrodes set in thermally matched glass, as illustrated in Fig. 3. Figure 4 illustrates the method of mounting the electrodes (transducer) in the pressure cell. The electrode-pressure cell combination is actually a cold cathode discharge tube that "fires" to conduct current under certain conditions. When the cell is fully pressurized, only a negligible leakage conduction occurs. If the cell leaks gas to a surrounding vacuum, as it would if penetrated by a micrometeoroid in space, the gas pressure will decrease until the electrodes can "break-down" or "fire" and conduct significant current. As pressure is further decreased, the conduction will extinguish and again become negligible. The term "transducer" will be used in the remainder of this report to refer to the electrode-pressure cell combination functioning as a cold cathode discharge tube.

Cold Cathode Discharge Tubes. - The electrical characteristics of a cold cathode discharge tube are a complex function of many variables including gas pressure; cathode geometry, material and surface conditions; temperature; gas properties; and the amount and type of ionizing radiation within the device. It is the Paschen characteristics of the pressure cells that are of special interest to the MDE Experiment. Generally, Paschen's law states that, for a given gas and cathode material and geometry, the firing voltage of a cold cathode device depends upon the product of gas pressure and electrode separation, i.e.,

$$V_f = f(px) \ ,$$

where V_f is the firing voltage, p is the gas pressure and x is the separation between the electrodes. Plots of V_f versus px are called Paschen curves. Since the electrode spacing (x) is controlled within specified limits by screening practices, Paschen curves for the MDE transducers are plotted with only pressure on the abscissa. A hypothetical Paschen characteristic is illustrated in Fig. 5 for the purpose of defining two important points. It is critical that the voltage applied to these transducers not exceed the firing voltage corresponding to the sealing pressure, V_{hi}, at any temperature. Secondly, it is critical that the applied voltage exceed the minimum firing voltage, V_{lo}, corresponding to any temperature. As a matter of good engineering practice, it is desirable that the pressurizing gas have Paschen characteristics with a large difference between V_{hi} and V_{lo}, and that the power supply voltage provide for a reasonable safety margin within these bounds. Consequently,

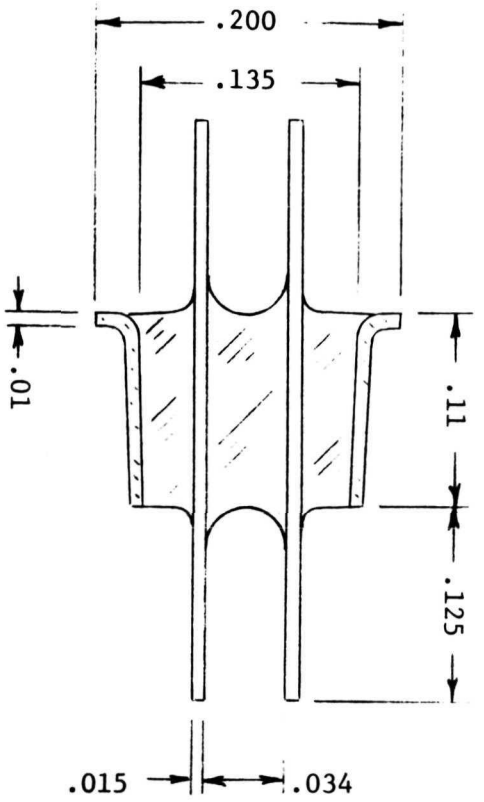

Fig. 3. Illustration of the MDE Transducer

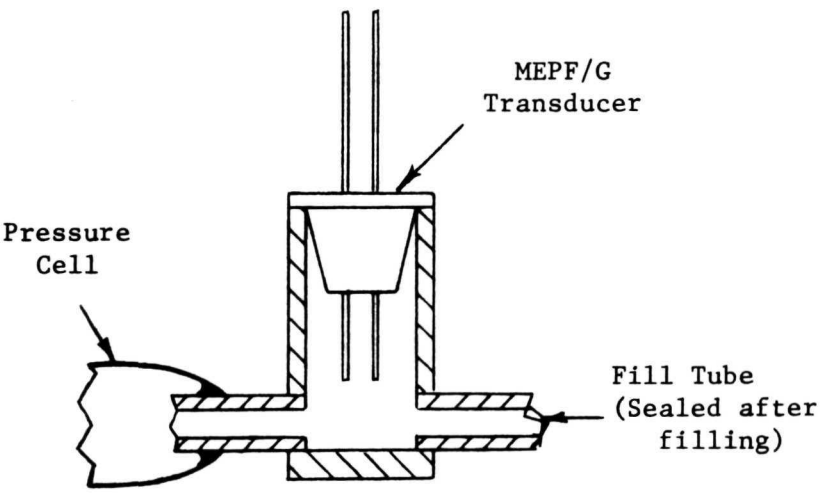

Fig. 4. Illustration of a Transducer Mounted in a Pressure Cell

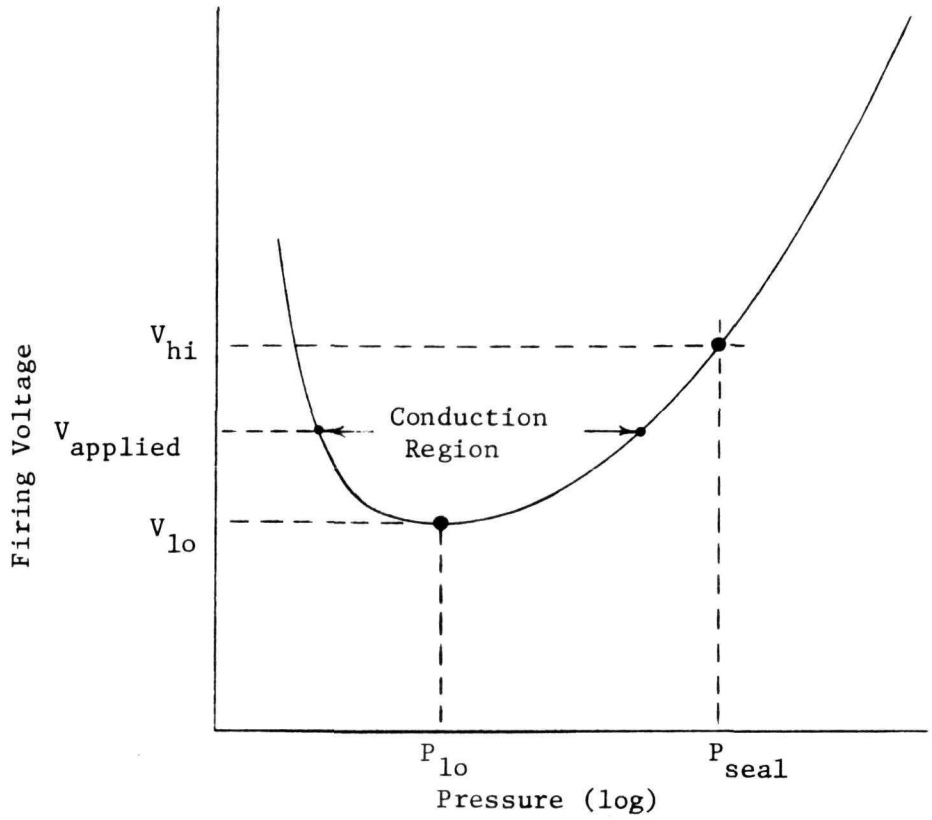

Fig. 5. A Hypothetical Paschen Characteristic

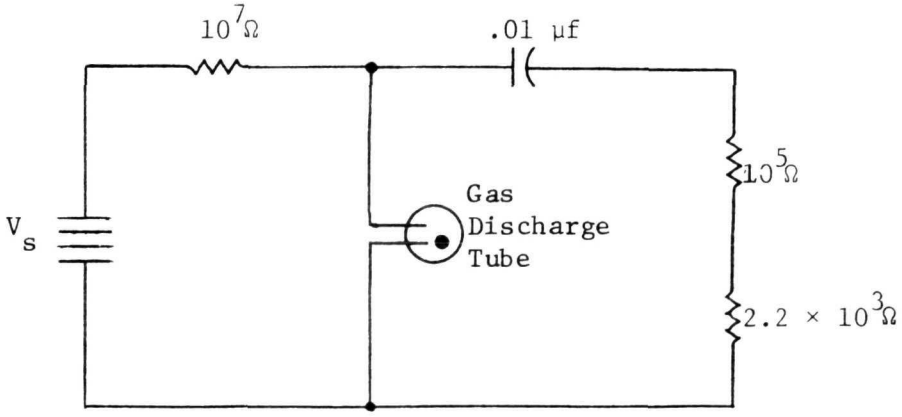

Fig. 6. Pressure Transducer Firing Circuit

the sealed MDE pressure cells have an applied voltage such that the transducers cannot fire and conduct current. In the event of a leak such as would occur to the vacuum of space if a cell were penetrated, pressure will decrease until a firing event can occur. As pressure continues to decrease, it will reach the low pressure intercept with the applied voltage, and no further firings or conduction can occur. Within the conduction region, power to the cell is limited by a series resistance as illustrated in the transducer circuit of Fig. 6. Energy to fire the cell and yield an output voltage is stored in the paralleled capacitor.

A source of initial ionization to insure reliable firing of the transducer whenever pressure-voltage conditions are favorable is provided by electroplating Ni^{63} on the transducer electrodes. It was found to provide for reliable operation of the transducer, but it does not otherwise influence the transducer's characteristics. The quantity of Ni^{63} deposited on each transducer is controlled by an electronic circuit described in Ref. 1, and by 100 percent screening of the plated units. The specifications regarding the quantity of Ni^{63} on each transducer largely reflect Pioneer Project specifications written to protect personnel and other experiments.

SECTION II

SUPPORTIVE INVESTIGATIONS

Paschen Curve Verification

The search for a gas that yields a Paschen characteristic suitable for the MDE Experiment was a significant activity under the preceding contract (NAS1-9420). A gas mixture of 75 percent Argon and 25 percent Nitrogen was selected, and Paschen curves for this gas were included in the final report [Ref. 1]. There was considerable uncertainty in the exact locus of the Paschen curves, and numerous data were recorded during this current effort to better define the curves. All of these data have fallen within the scatter of data previously determined. Figure 7 includes experimental Paschen curve data for the possible combinations of temperature and electrode geometry and surface conditions. As illustrated, these data tend to fall into two groups, i.e., room temperature and liquid Nitrogen temperature data. Other than temperature, variations in electrode space, electrode surface roughness and nonuniformities at the electrode ends due to a cutting operation contributes to the scatter. Additionally, the firing process is a statistical process and some scatter is inherent. The significant feature of these data is that the pressure-cell sensor is demonstrated to be suitable for the MDE Experiment and a large safety margin exists. The Paschen curve for a given pressure-cell could fall significantly outside the shaded region of Figure 7 without compromising the MDE Experiment.

Nickle-63 Variations

A significant achievement under NAS1-9420 was the selection of Ni^{63} as a suitable source of initial ionization for the MDE pressure cells. Permissible quantities of Ni^{63} were demonstrated to provide for reliable operation of the pressure transducers.

The quantity of Ni^{63} deposited on the MDE electrodes was limited by Pioneer Project specifications that allotted the entire experiment a total of 1 μCi of radioactivity [Ref. 2]. A total of 13 panels of 18 cells each had to share this total quantity. Consequently, 0.003 μCi of Ni^{63} was selected as nominal for each cell, thus providing an adequate safety margin below the 1 μCi limit. An obvious question for consideration concerned the criticality of the quantity of Ni^{63} in use to the reliable operation of the MDE transducers. Specifically, was the quantity in use near some critical minimum such that reliability might be adversely affected?

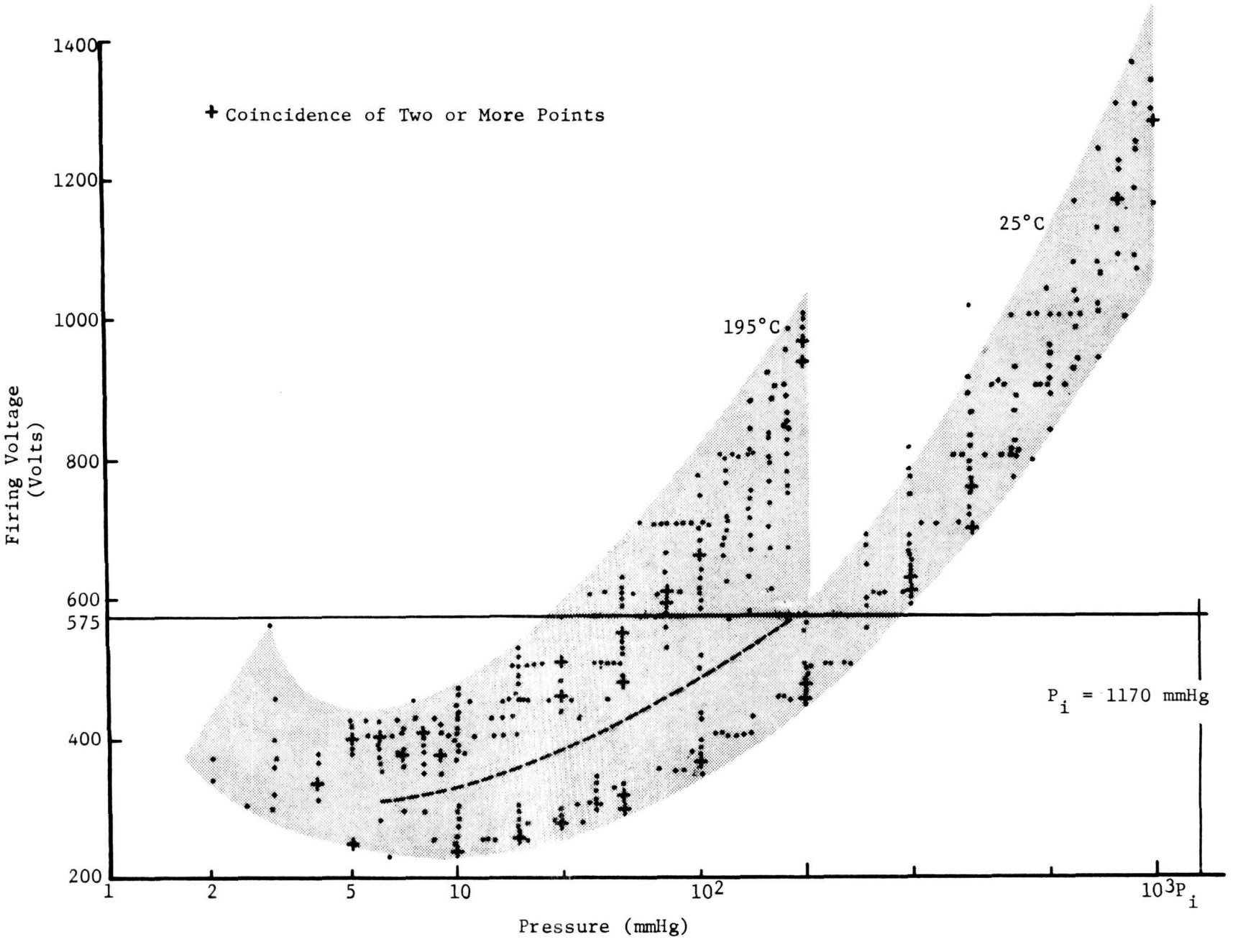

Fig. 7. MDE Paschen Characteristics

The cleaning, plating and counting procedure for controlling the quantity and quality of the Ni^{63} plate deposited on the MDE electrodes has been described [Ref. 1]. The quantity is controlled by 100 percent screening of the plated units. Acceptable quantities range from 0.00255 to 0.00345 μCi, or 4245 to 5778 disintegrations/minute. From the definition of a curie, i.e.,

$$1 \text{ Ci} \equiv 3.7 \times 10^{10} \text{ disintegrations/sec.},$$

and assuming the worst case of 0.00255 μCi, it can be calculated that, on the average, 94.5 electrons per second will be available to initiate this ionization process, i.e.,

$$0.00255 \text{ μCi} = 94.5 \text{ disintegrations/sec} .$$

It has been estimated that the most rapidly decaying MDE pressure cells will find conditions favorable for conduction for a period ranging from 0.01 to 0.1 seconds, and only 1.4 percent of the 98.7 percent of the cell-leak events accounted for in the estimate will be that low [Ref 3]. Consequently, it is estimated that an average of from 0.945 to 9.45 electrons will be available to start the ionization process for the worst-case situation. (Practically all of the betas have sufficient energy to initiate the ionization process.) Confidence that the amount of Ni^{63} committed to the MDE transducer is adequate is further enhanced by estimates of the time required to exhaust the volume of gas trapped in the vicinity of the electrodes through the small tube connecting this volume with the pressure cell. For a closed volume of gas connected by a tube to a perfect vacuum, the following expression is derived by Dushman [Ref. 4]:

$$\frac{1}{b}\left(\frac{1}{P_2} - \frac{1}{P_1}\right) = t_2 - t_1 = \Delta t,$$

where

$$b = 0.0736 \, aF_5/cV ,$$

and

$$F_t = 30.48 \, a^3/\left(\frac{T}{M}\right)^{1/2} .$$

Further,

P_1 = pressure at t_1 (μbars) ,

P_2 = pressure at t_2 (μbars) ,

$P_1 > P_2 \geq 100$ bars ,

$t_2 > t_1$,

V = volume to be evacuated (cm^3) ,

a = radius of tube (cm) ,

c = mean free path at 1 μbar ,

ℓ = length of tube (cm) ,

T = absolute temperature (°C) ,

and

M = molecular weight of the gas .

Using worst-case values descriptive of the MDE experiment, i.e.,

P_1 = 100 mmHg = $10^7/75$ μbars ,

P_2 = 1 mmHg = $10^5/75$ μbars ,

a = 3.8×10^{-2} cm ,

V = $0.00\ 2 \times (2.54)^3$ cm^3 ,

c = 6.78 cm (Dushman, for air at 25°C, 1 μbar) ,

T = 300°K ,

and

M = 28 (N_2) ,

the time to reduce pressure from 100 mmHg to 1 mmHg calculates to 22 seconds. It is concluded, therefore, that the quantity of Ni^{63} used in each transducer is sufficient. Experimentally, it has not been possible to induce failures by arranging rapid leak rates.

Another consideration relative to the optimum amount of Ni^{63} is that betas emitted from the cathode and arriving at the anode (or the transducer housing) constitute a leakage current. If it is assumed that the maximum permissible amount of Ni^{63} is on the cathode and that each beta arrives at the anode, a worst-case leakage current can be calculated as follows:

$$0.00347\ \mu Ci = 128 \text{ electrons/sec} ,$$

$$1 \text{ ampere} \equiv 1 \text{ Coulomb/sec} = 6.24 \times 10^{18} \text{ electrons/sec} ,$$

Therefore,

$$0.00347\ \mu Ci = \frac{128}{6.24 \times 10^{18}} \simeq 2.1 \times 10^{-16} \text{ amperes} .$$

This current would correspond to a power drain across 234 paralleled cells with 1000 volts applied of less than 5×10^{-12} watts or a voltage drop across the $10^{7}\Omega$ resistor in the transducer circuitry of less than 5×10^{-8} volts. Therefore, leakage due to the presence of the Ni^{63} is negligible.

Experimentally, Ni^{63} variations have been investigated by determining the Paschen characteristics of a series of transducers plated with quantities of Ni^{63} that differ significantly from the nominal 0.003 μCi. These five transducers have quantities of Ni^{63} from approximately 0.1 to 3 times nominal value. Resulting Paschen curves at both 25°C and LN_2 temperatures are essentially unchanged from the standard 0.003 μCi units. All of these units were tested after several hours of storage at LN_2 temperatures and there were no incidents of failure-to-fire.

The Paschen curve data descriptive of these five transducers are presented in Figs. 8 and 9 for room and liquid nitrogen temperature, respectively. These data were determined using a standard procedure. The transducer circuit of Fig. 6 was used, the gas pressure was held constant, and voltage was increased until a firing event occurred.

Hole Size Considerations

Weight and power limitations imposed by Spacecraft capabilities circumvented any MDE designs to yield hole size information. One possible approach would be to utilize the period of the oscillating transducer as a measure of the leak rate. This would require that the conduction impedance vary in a predictable manner with gas pressure and that the conduction period be a significant part of the total period of oscillation.

The conduction impedance of the MDE transducer was measured by observing its I-V characteristics in the continuous glow circuit of Fig. 10. The voltage across R_2 was recorded with a dual channel strip

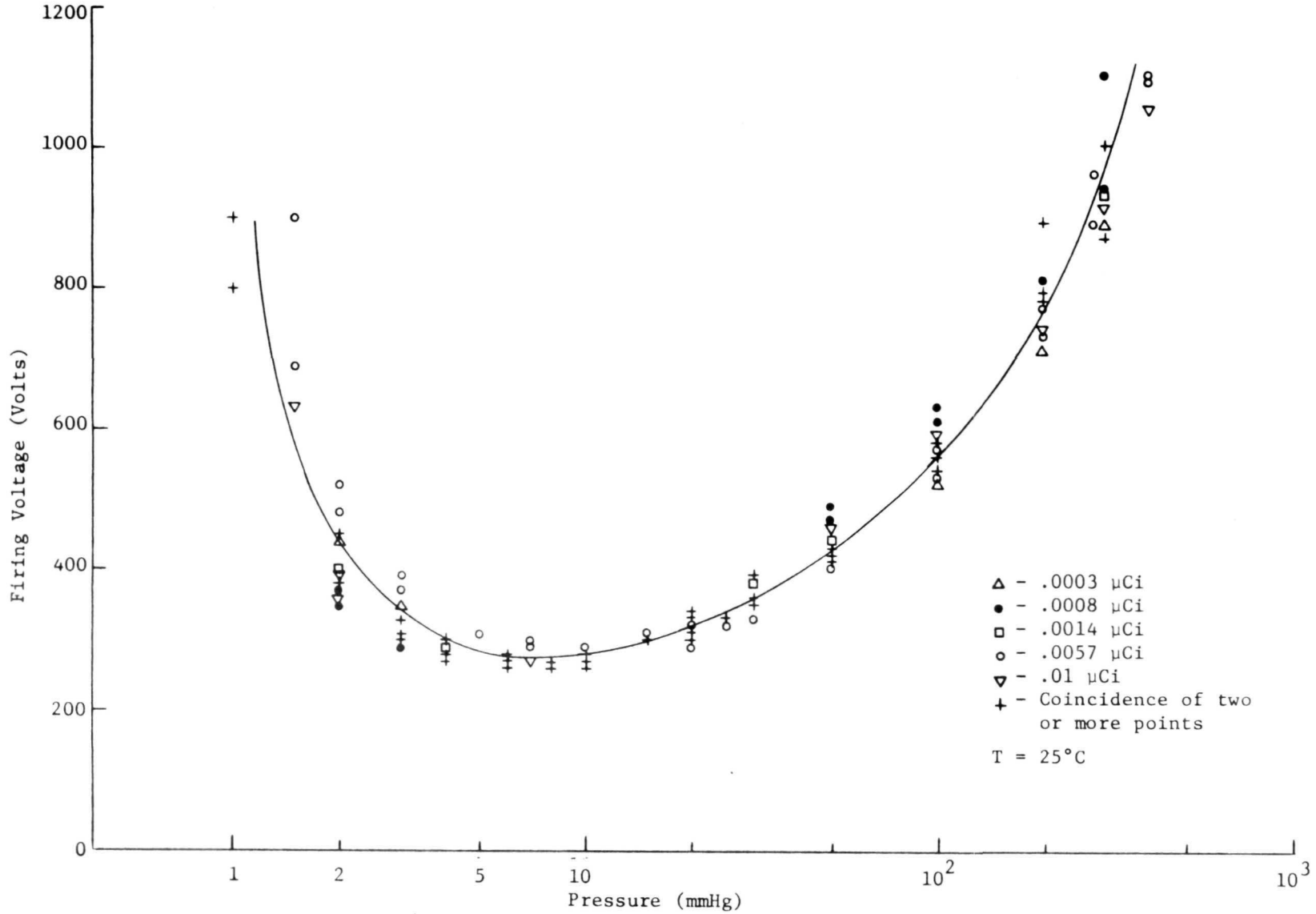

Fig. 8. MDE Paschen Characteristics with Varied Quantities of Ni^{63}, T = 25°C.

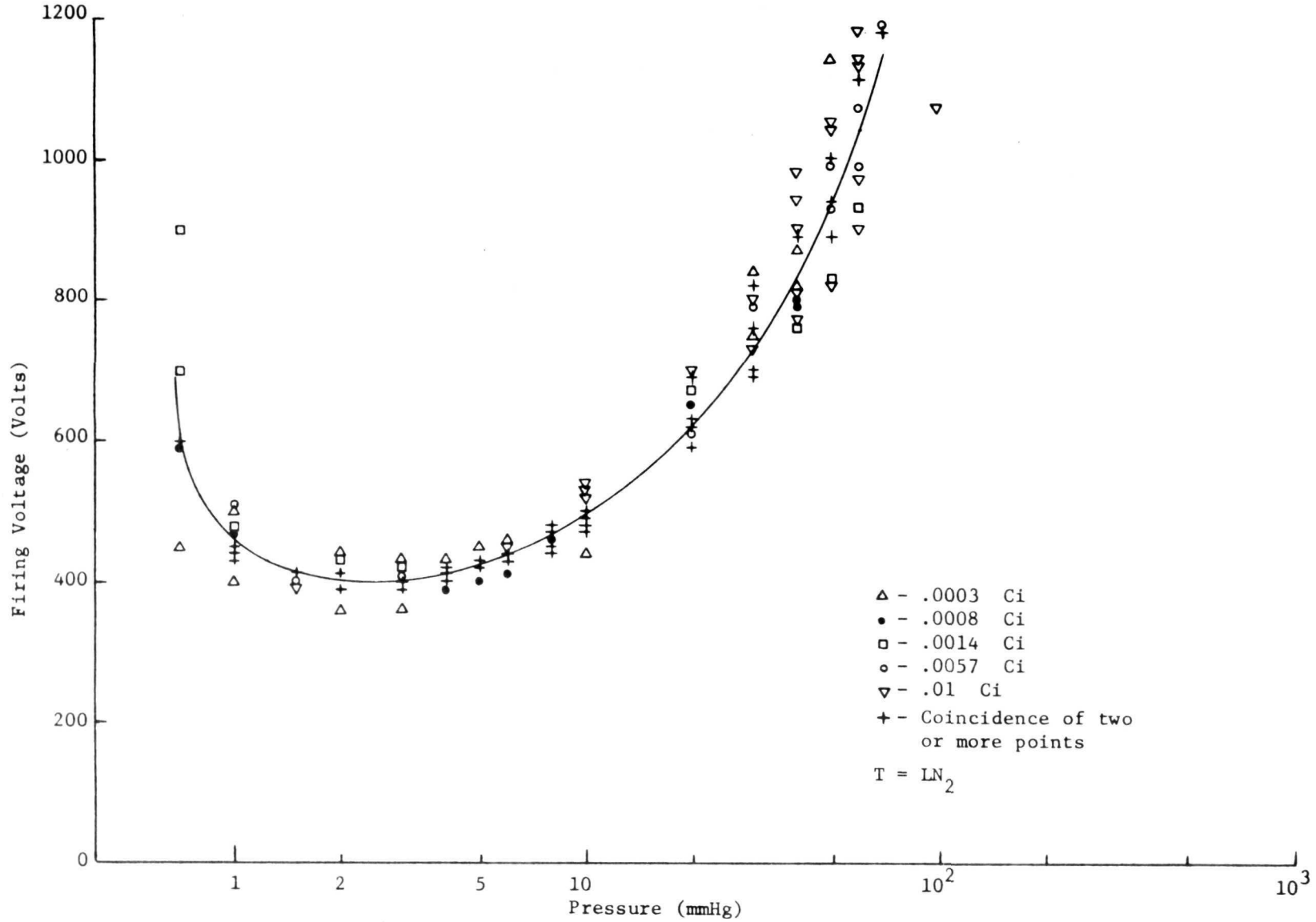

Fig. 9. MDE Paschen Characteristics with Varied Quantities of Ni^{63}, T = -195°C

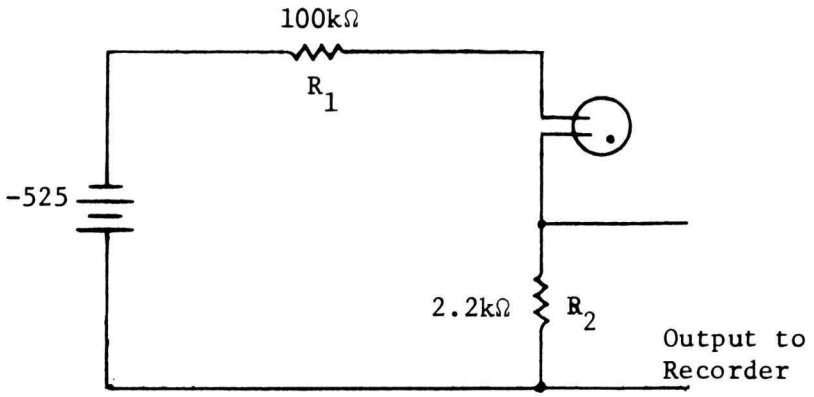

Fig. 10. Continuous Glow Circuit

chart recorder. The pressure in the cell was recorded on the second channel, i.e., on the same time base. At any pressure, V_{R2} can be read from the recorder and the conduction impedance, R_T, calculated from

$$R_T = V_T/I = \frac{1}{I} [525 - (V_{R1} + V_{R2})] ,$$

where

$$I = V_{R2}/R_2 ,$$

$$V_{R1} = IR_1, \text{ and}$$

$$V_T = \text{transducer voltage.}$$

Following this procedure, the conduction impedance curves of Fig. 11 were determined. Because of the difficulty of reading pressure from the recorder, there is considerable uncertainty in the curves generated. It is observed, however, that the conduction impedance varies considerably with pressure, beginning at approximately 100 kΩ at 100 mmHg and increasing to approximately 1000 kΩ before conduction ceased. (It was significant to observe that conduction had always ceased when pressure reached 2 mmHg.)

Another useful observation concerned the period between the first and second firing events, for example. These periods varied significantly, especially at low leak rates, and often lasted for several minutes.

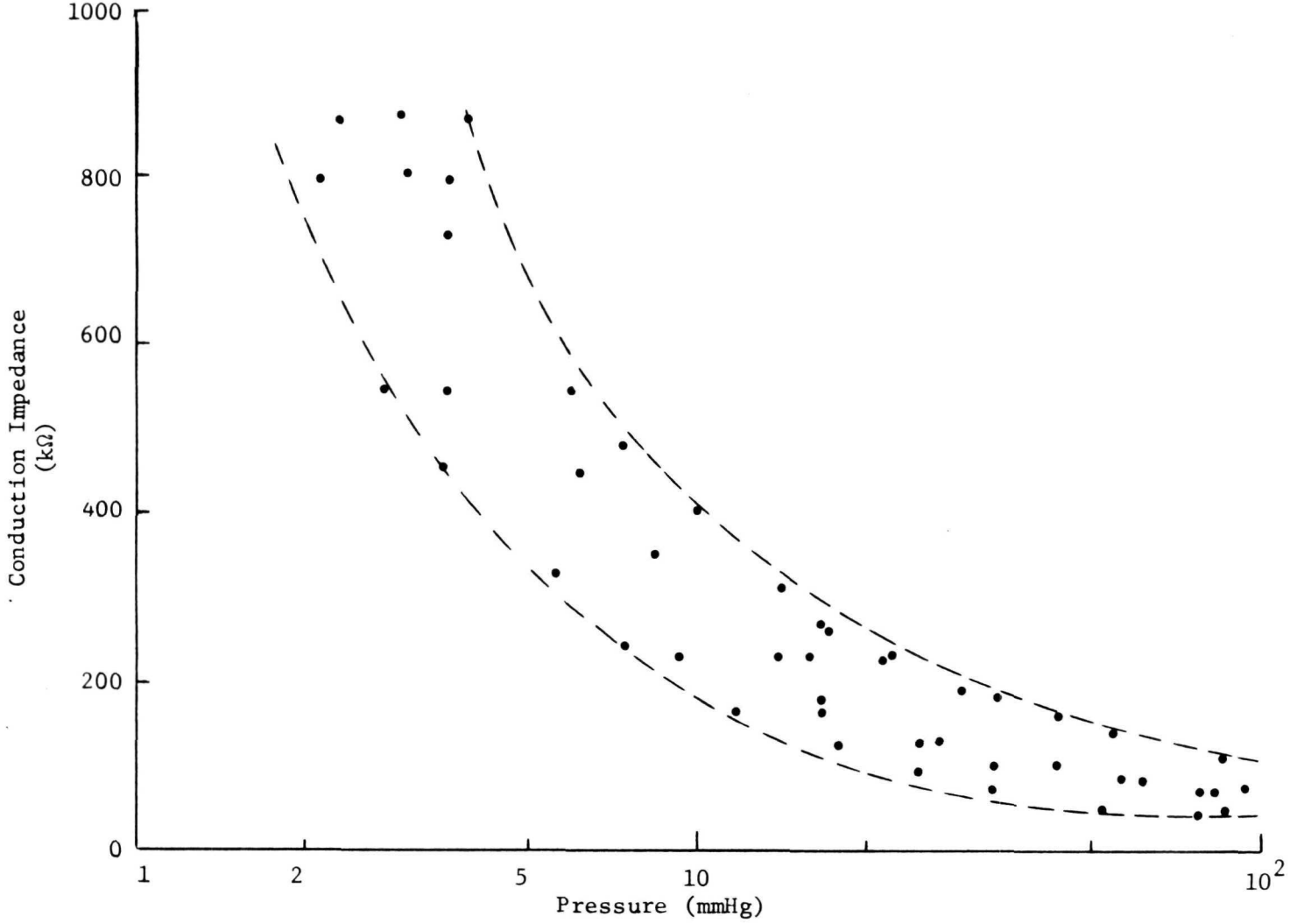

Fig. 11. Conduction Impedance Versus Pressure.

If the MDE experiment were reconfigured to yield hole size information, power would still be a critical factor and a power limiting circuit such as the MDE circuit would be required. In this circuit, the output signal largely reflects the circuit parameters. However, the output pulse shape, frequency and width vary significantly as pressure changes. This suggests that hole size information can be obtained if the appropriate circuitry is added. The oscillograms of Fig. 12 are included as an example of the variations that occur in the output of a single transducer. There is also considerable variations between transducers. Much data of this type has been recorded, and it is concluded that the transducers will have to be made more uniform if a hole size capability is to be added to the MDE system.

Sputtering Study

To investigate the possibility of test firings sputtering electrode material and changing the pressure cell characteristics, a sample of cell-mounted transducers were forced to sputter in a continuous glow circuit that permitted approximately 1 watt of dissipation across the transducer for several seconds. The glow circuit is illustrated in Fig. 13. Afterward, leakage impedances were checked and observed to be still above the 10^{14} Ω measurement limit, indicating that sputtered material had not created a significant metal film path between the electrodes, and the firing voltages of the cells were observed to be approximately the same. The transducers were then removed from their housings and examined under a microscope for evidence of sputtering. In the most severe cases, the electrode surfaces, both anodes and cathodes, had a different finish, indicating that some sputtering had occurred. Finally, the radioactivity of the transducers was measured and compared with previous readings. The cathodes were then removed and the anodes recounted. These results, tabulated in Table I, do not show any significant differences between the electrodes. These results also indicate that sputtering of electrode material, including the Ni^{63} electroplate, did occur. Increasing the power dissipated or time did not significantly influence the results. This suggests that the sputtering became localized on the electrodes and continued in the same area.

It is significant that although power dissipation in this sample was increased such that sputtering was caused to occur, it did not degrade the pressure cells performance. It is concluded, therefore, that the pressure cells can be fired in numerous tests without causing any degradation due to sputtering.

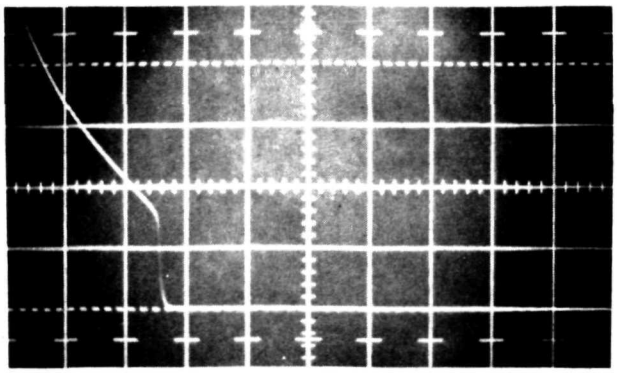

1st Pulse
100 mmHg
1 V/div.
0.5 ms/div.

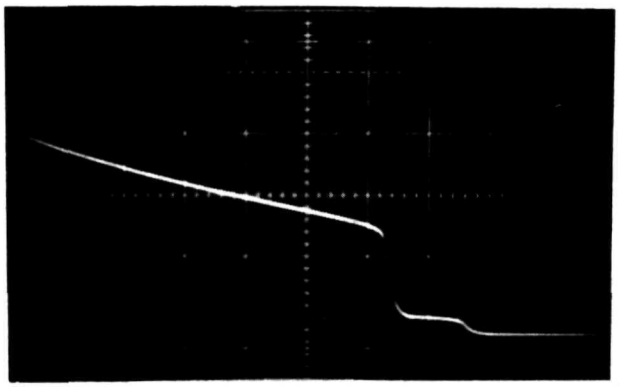

14.5 mmHg
0.2 V/div.
2 ms/div.

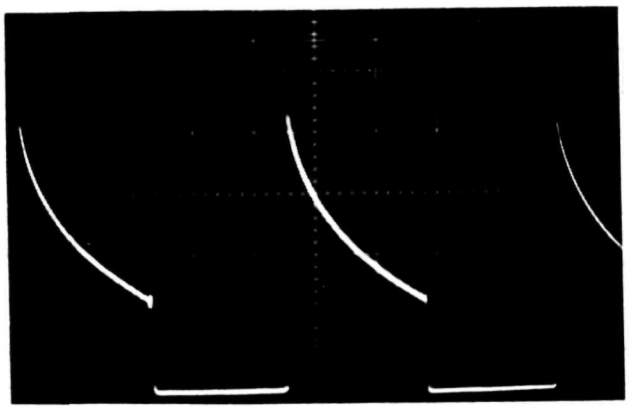

7 mmHg
0.05 V/div
2 ms/div.

Fig. 12 Oscillograms of the Output Pulse of an MDE Transducer

Table I

Sputtering Study Results

Transducer	Power Dissipated (Watts)	Time (Seconds)	Radioactivity (mμ Ci)		
			Initial	After Sputtering	Anode Only
1	.76	15	3	.8	.4
2	.76	30	3	.7	.3
3	1.4	15	3	.9	.6
4	1.4	30	3	.8	.4
5	1.4	120	3	.8	.4

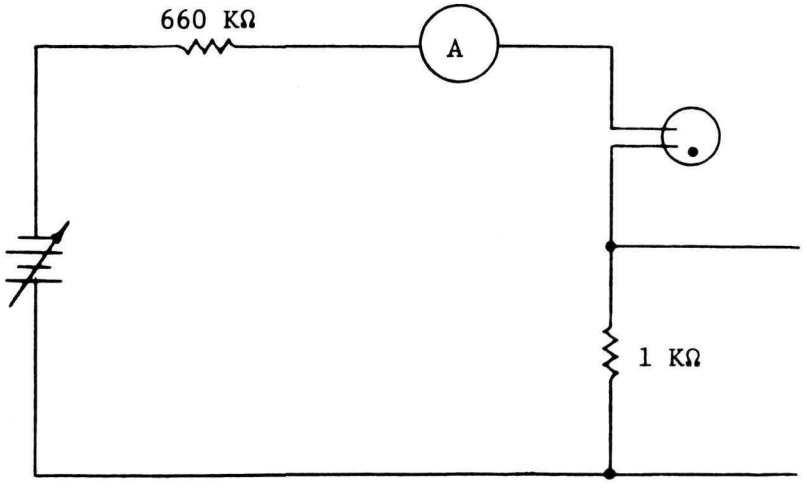

Fig. 13. Continuous Glow Circuit

Geometry Variations

A sample of four transducers was modified to the U-shaped and spark-plug geometries illustrated in Fig. 14. These were plated with Ni^{63}, mounted in the usual housing and their Paschen characteristics were determined. These results are shown in Fig. 15, and the "nominal" Paschen characteristics are shaded in for comparison purposes. The U-shaped units had spacings of 20 and 30 mils, and the spark plug units had spacings of 30 and 40 mils. The Paschen characteristics of these units are not unlike the characteristics of the nominal MDE transducer. The generally lower firing voltages may be due to increased electric field values caused by increased imperfections or "roughness" on the mechanically shaped electrodes. The slight lowering of the curve at higher pressures without a comparable lowering of the curve minimum is also a less desirable characteristic than the nominal.

The advantages of continuing these investigations into geometrical effects is marginal without making significant improvements in such geometrical factors as uniformity of spacings and surface finishes.

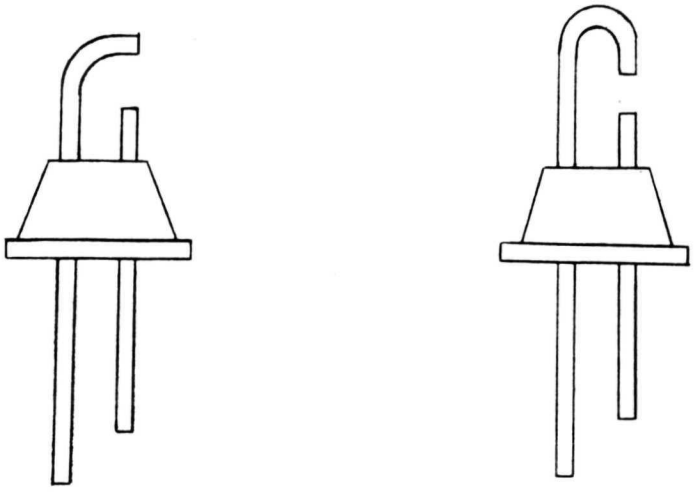

Fig. 14. Altered Electrode Geometries

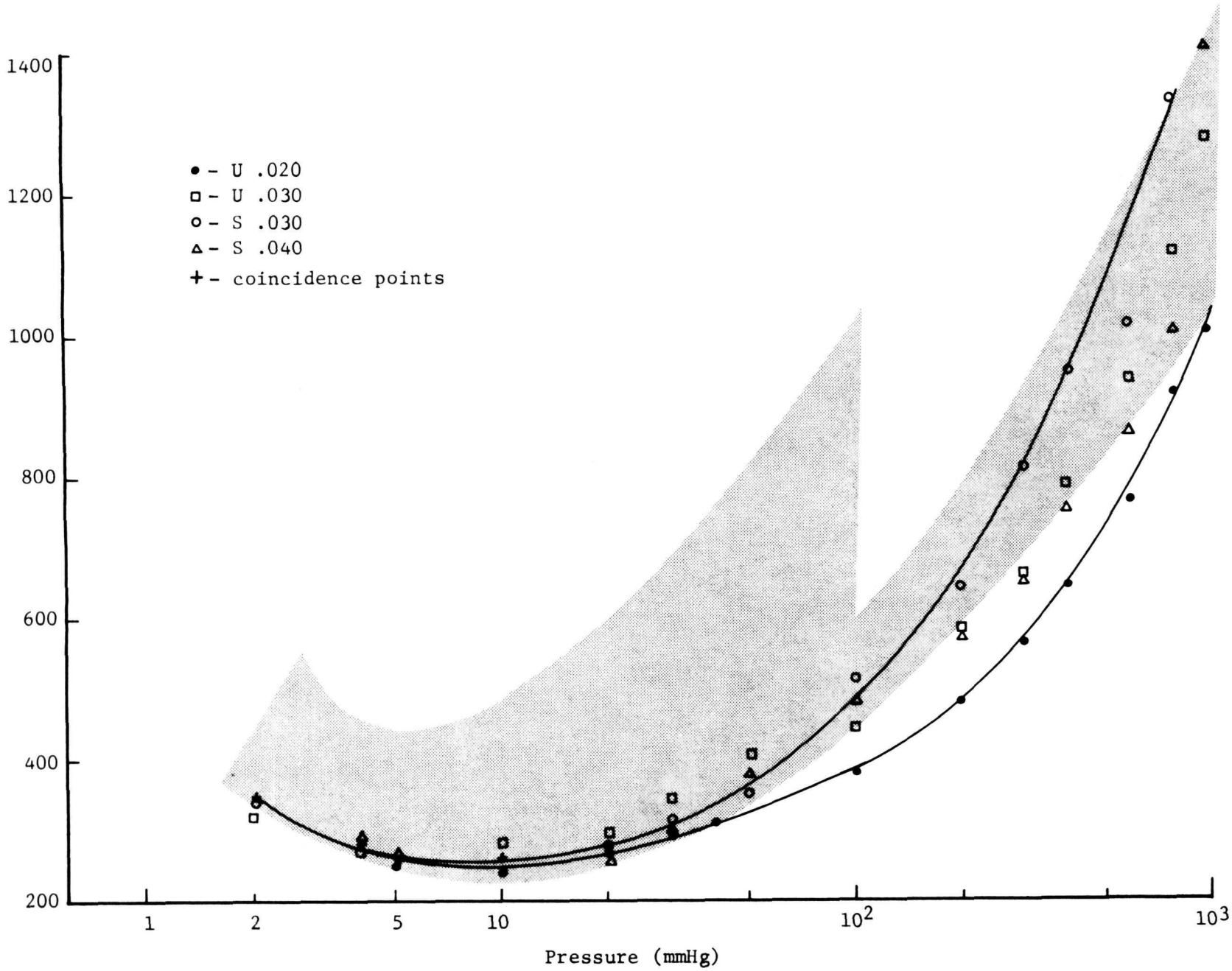

Fig. 15. Paschen Characteristics of MDE Transducer with Altered Geometries.

Ni^{63} Plating Results

The Ni^{63} plating procedure and apparatus is described in detail in Ref. 1. Electrode plating was continued into the current program with continuing excellent results. Approximately 4500 transducers were plated and individually counted. A histogram of the counted values is shown in Fig. 16. Those units outside the $\pm$ 15 percent of nominal value marks were rejected and not delivered for use on the MDE.

Two Ni^{63} plated transducers were counted at every opportunity by including them in a group of transducers going through the counting procedure. These check units were counted approximately 30 times, and the counts varied $\pm$ 2 percent about the nominal value.

Influence of External Radiation

There was concern that ionized particles encountered in space with energies in the GeV range would produce holes in the pressure panels which would allow the pressurizing gas to leak out or otherwise cause the pressure transducer to fire. Dr. Thomas S. Elleman of North Carolina State University, an authority on radiation damage in materials, was consulted on the question of ionized particles producting holes in the panels. It was concluded, from studies of radiation damage induced by fission fragments, that penetrations by ionized particles would not be a problem. It is reasonsed that if the thickness of the penetrated materials is at least an order of magnitude greater than the diameter of the penetrating particle, then sputtering on either side of the penetrated material will not leave a hole completely through the material. The material in the vicinity of the trajectory will exhibit a high density of dislocations and can be easily removed by etching. However, there will be no voids through which the pressurizing gas can escape.

An ionized particle penetrating a panel can be simulated by placing a thin piece of the panel material in contact with a slab of enriched uranium (U^{235}) in a nuclear reactor. The reactor neutrons would cause the uranium slab to fission and hence bombard the panel material with high energy fission fragments. The maximum thickness of stainless steel which fission fragments will penetrate is approximately 1/4 mil. It would be a relatively difficult task to subsequently inspect the material since it would be radioactive.

The possibility of external radiation causing a cell to fire has also been investigated. From the I-V characteristics of a pressurized cell, it was noted that a cell could not be maintained in a "glow" condition at current levels less than 10^{-4} amps. This suggests that an ionizing event in the vicinity of the electrodes of a pressurized cell must produce enough

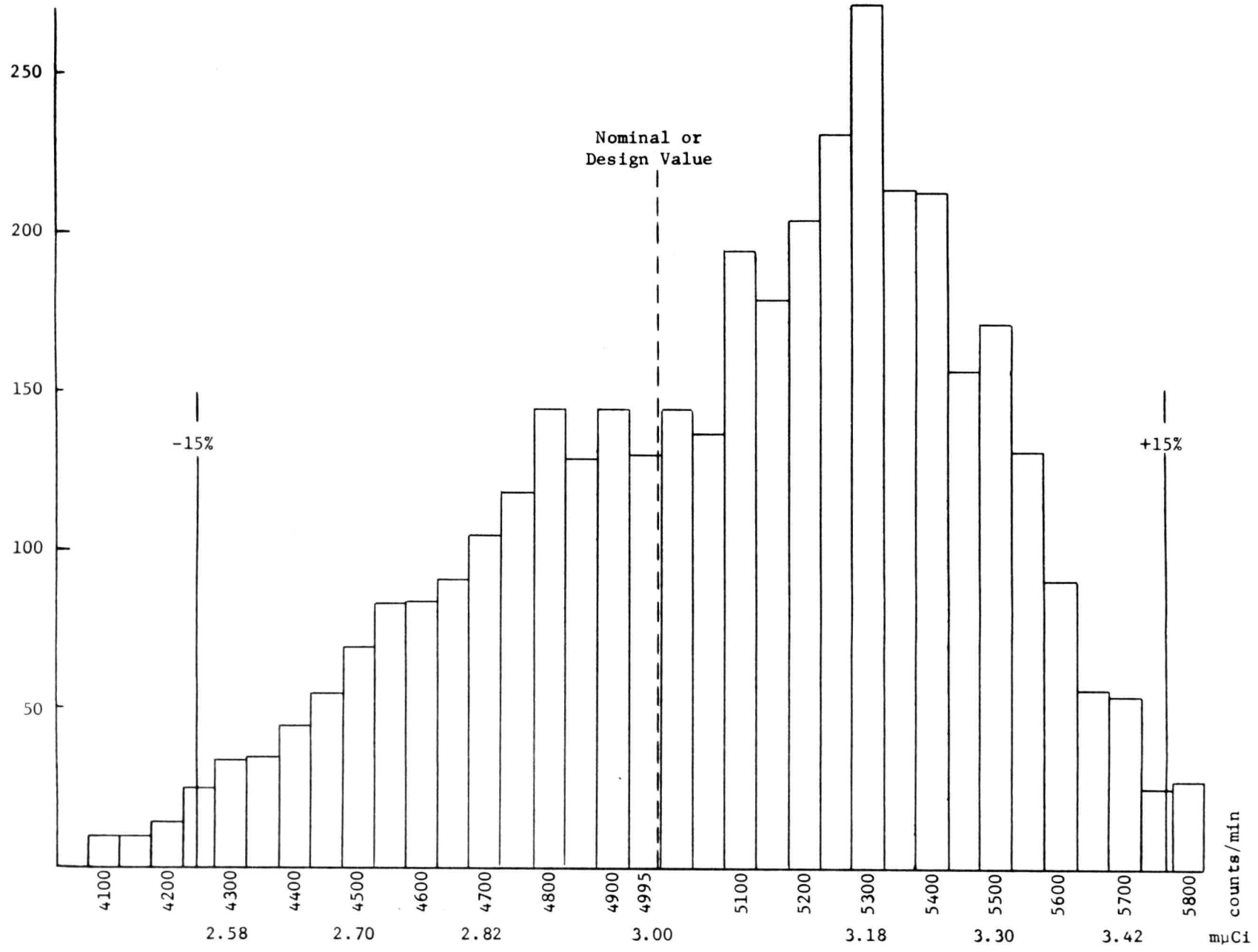

Fig. 16. Histogram of Ni^{63} Plating Results

ions to yield a current of approximately 10^{-4} amps. If it is assumed that 1 BeV particles yield 15 MeV energy in the cell, for example, it would require approximately 10^{9} particles per second to produce 10^{-4} amps. An ionization energy of 15 eV is required to ionize the gas. Even with gas multiplication of 10^{4}, 10^{5} particles per second would be required.

Experimentally, a sealed electrode was exposed to a gamma dose rate of 1.7×10^{11} eV/s by placing it adjacent to 1.5 kCi of Co^{60}. This corresponds to a current level of 10^{-9} amps without gas multiplication. There was no reduction in the 1400 volts firing voltage.

Subsequent to these investigations, the NASA SREL facility was utilized to simulate the proton and heavy ion environment of space, and the MDE transducers were tested in the simulated environment. These tests and test results are discussed in Appendix B of this report.

Appendix C discusses the effects of the proton and heavy ion environment on an MOS capacitor-type meteoroid detection transducer.

Page Intentionally Left Blank

SECTION III

DEVELOPMENT PANEL TEST PROGRAM

Initial efforts to monitor the firing voltages of development pressure panels over extended time intervals showed a significant, somewhat reversible reduction in firing voltages when the panels were placed in a vacuum. If left in a vacuum, the firing voltages would continue to decrease with time over a period of several days. These characteristics were due to a yielding of the pressurized cells which increased their volume, lowering pressure and gas density of the sealed cells. In response to these observations, the sealing pressure was increased from 16.7 PSIA to 22.7 PSIA and the panels were screened to reject any panels with firing voltage below 1000 volts.

Tables II and III are included to illustrate the firing voltage characteristics of many of the development panels. Panel No. 025, Table II, is typical of the first panels. These were placed on a routine test schedule, and the voltage degradation became apparent as data became available. Table III shows similar results for another of the development panels. In each case, the initial firings in an ambient pressure of 14.7 PSIA and in a vacuum are included, and also the final firing in a vacuum as these panels were removed from further tests.

In Table IV firing voltages in another development panel, Panel No. 063, over a period of several days are tabulated along with the average value of the firing voltage at each firing period. These results, again, show a large, reversible firing voltage decrease whenever the panel is placed in a vacuum, but the continuing decrease is not significant as it was in some earlier panels. Tables V and VI tabulate similar results for Panels No. 064 and 065, respectively, except only a few, evenly spaced-in-time firings are included.

During the course of testing panels and reviewing data, it became apparent that a disproportionate number of panels fired on integral hundreds of volts. The only explanation for this phenomenon was that in the process of increasing the applied voltage, it was inherent in the procedure that the power supply was switched to an integral hundreds of volts slightly longer than on the interim decades. Consequently, a timer was added to the firing procedure and each voltage increment was held for five seconds. This procedure probably improved the uniformity of the data somewhat. Since the firing procedure is statistical in nature, it is reasonable that uniformity would be enhanced by timing the switching of voltage increments.

In view of the flexibility of the stainless steel panels, the large, reversible change that occurs in firing voltage depending upon whether the cell is in an ambient vacuum or one atmosphere is reasonable. If a

Table II

Firing Voltages of Panel No. 025

Cell No.	Initial Firing p = 14.7 PSIA) 12/18/70 (Volts)	Initial In Vacuum p < 10 μHg 12/18/70 (Volts)	p < 10 μHg 2/19/71 (Volts)
1	1340	1140	990
2	1615	1210	1180
3	1585	1010	930
4	1515	910	900
5	1516	1050	1000
6	1666	1110	1010
7	1460	1195	1100
8	1417	1025	1040
9	1660	1150	1060
10	1660	1250	1140
11	1430	1095	970
12	1565	1013	930
13	1673	920	980
14	1455	880	920
15	1588	1210	1100
16	1645	1143	1090
17	1603	1050	1050
Average	1552	1080	1022

Table III

Firing Voltages of Panel No. 044

Cell No.	Initial Firing (p = 14.7 PSIA) 1/27/71 (Volts)	Initial In Vacuum p < 10 μHg 1/27/71 (Volts)	p < 10 μHg 2/12/71 (Volts)
1	1300	710	610
2	1350	710	700
3 3	1460	820	790
4	1400	790	840
5	1420	900	830
6	1550	730	660
7	1530	850	770
8	1330	850	700
9	1410	1060	860
10	1320	900	860
11	1330	800	790
12	1550	930	830
13	1500	820	800
14	1370	990	880
15	1430	1000	990
16	1460	940	870
Average	1419	862	792

Table IV

Firing Voltages of Panel No. 063

Cell No.	Initial Firing (p = 14.7 PSIA) 2/19/71 (Volts)	Initial In Vacuum p < 10 μHg 2/22/71 (Volts)	p < 10 μHg 2/22/71 (Volts)	p = 14.7 PSIA 2/22/71 (Volts)	p < 10 μHg 2/23/71 (Volts)	p < 10 μHg 2/24/71 (Volts)	p = 14.7 PSIA 2/25/71 (Volts)	p < 10 μHg 2/26/71	p < 10 μHg 3/1/71	p < 10 μHg 3/4/71
1	1200	820	780	1200	770	790	1080	780	800	720
2	1390	790	740	1300	760	770	1200	800	840	770
3	1300	860	900	1200	700	710	1050	720	750	780
4	1300	800	810	1290	820	870	1290	870	880	880
5	1220	790	830	1210	730	760	1000	650	710	700
6	1210	830	830	1290	810	870	1170	810	820	870
7	1250	830	750	1200	790	780	1100	800	800	800
8	1360	930	770	1200	800	790	1200	830	810	820
9	1390	920	890	1300	860	900	1300	890	890	890
10	1300	850	820	1110	800	840	1130	820	840	850
11	1480	780	730	1200	690	690	1030	700	700	730
12	1510	800	780	1100	800	800	1030	730	770	730
13	1440	790	750	1170	730	720	1020	770	790	760
14	1310	800	750	1200	770	800	1100	770	800	740
15	1530	830	780	1140	770	750	1100	740	790	770
16	1350	800	790	1120	800	780	1110	790	800	800
17	1400	870	840	1300	870	850	1300	850	840	830
Average	1350	830	796	1149	780	786	1130	783	801	790

Table IV (Continued)

Firing Voltages of Panel No. 063

Cell No.	p = 14.7 PSIA 3/5/71 (Volts)	p < 10 μHg 3/5/71 (Volts)	3/5/71 (Volts)	3/11/71 (Volts)	3/12/71 (Volts)	3/18/71 (Volts)	3/22/71 (Volts)	3/22/71 (Volts)	3/29/71 (Volts)	4/8/71 (Volts)	p = 14.7 PSIA 4/8/71 (Volts)
1	1100	800	900	770	760	750	740	740	740	720	1100
2	1180	800	800	760	780	750	760	760	740	740	1200
3	1090	710	800	700	720	750	750	750	720	730	1000
4	1300	860	860	880	890	860	880	880	890	860	1300
5	1020	620	620	700	700	680	670	670	690	700	900
6	1230	800	800	840	820	840	850	850	880	860	1180
7	1130	790	790	800	790	800	780	780	780	780	1110
8	1110	800	800	800	800	800	840	840	850	820	1110
9	1300	880	880	900	880	900	900	900	900	890	1300
10	1120	820	820	900	820	800	810	810	810	840	1110
11	1000	690	690	690	690	660	690	690	700	690	940
12	960	700	700	740	680	730	710	710	720	720	990
13	1040	740	740	740	770	730	730	730	750	770	1080
14	1200	790	790	800	800	750	750	750	790	740	1170
15	1070	800	800	770	770	780	800	800	800	770	1170
16	1200	800	800	830	800	830	800	800	830	800	1140
17	1300	840	840	840	830	850	840	840	840	840	1320
Average	1138	778	779	792	782	780	782	782	790	780	1124

Table V

Firing Voltages of Panel No. 064

Cell No.	Initial Firing (p = 14.7 PSIA) 2/19/71 (Volts)	Initial In Vacuum 2/20/71 (Volts)	p < 10 μHg 2/26/71 (Volts)	3/5/71 (Volts)	3/22/71 (Volts)
1	1970	1260	1040	1110	1000
2	1880	1060	810	740	700
3	1370	1060	730	730	700
4	1530	980	700	780	820
5	1600	1140	860	830	820
6	1400	1060	800	700	710
7	1440	1030	700	660	700
8	1490	920	710	930	700
9	1680	1100	900	940	930
10	1400	1070	890	880	850
11	1360	1050	870	880	700
12	1460	810	780	640	670
13	1610	1040	900	900	890
14	1530	800	720	890	700
15	1510	810	620	650	790
16	1470	900	850	900	870
17	1520	930	890	940	870
18	1490	900	660	670	740
Average	1539	996	801	820	787

Table VI

Firing Voltages of Panel No. 065

Cell No.	Initial Firing (p = 14.7 PSIA) 2/19/71 (Volts)	Initial In Vacuum 2/25/71 (Volts)	p < 10 μHg 2/26/71 (Volts)	3/15/71 (Volts)	3/22/71 (Volts)
1	1290	950	830	830	810
2	1400	1040	930	960	950
3	1400	1160	900	850	910
4	1350	1090	970	950	930
5	1360	1060	900	910	900
6	1450	1130	930	900	920
7	1300	1130	890	910	900
8	1280	1030	880	860	900
9	1410	1100	910	830	800
10	1470	1080	920	890	880
11	1420	1080	890	840	830
12	1510	1040	910	940	940
13	1480	1130	930	990	950
14	1490	1090	900	900	890
15	1450	1080	900	900	900
16	1440	1020	900	930	900
17	1540	1090	950	930	920
18	1400	940	810	800	790

pressurized cell has an atmosphere of pressure pressing it and is then immersed in a vacuum, it is reasonable that it will expand. The cell can be observed to increase in volume as the ambient surrounding it is evacuated. It is estimated from an empirical procedure that a cell expanding from a reasonably pillowed shape to a near circle will expand in volume, thus reducing pressure and gas density, by a factor of 2.5.

Flight-Type Panel Test Results

The LRC fabrication facilities responded to all development panel test results and produced pressure panels with characteristics suitable for the MDE Experiment. Table VII is a history of the first of these flight-type panels committed to long-term testing, Panel No. 092. As with previous panels, a reduction in the firing voltage occurs when the panels are placed in an ambient vacuum. However, as is evident in the data tabulated in Table VII, the in-vacuum voltages of these panels are satisfactory and very uniform. Data comparable to the results from Panel No. 092 were obtained from numerous other panels, e.g., Panels 075, 076, 077 and 084. Of these, Panel No. 075 was tested more extensively than No. 092 and yielded excellent, uniform results.

Table VII is included in this report with reluctance because of its extensiveness. However, Panel 092 is a flight quality panel that received extensive testing and was included in the long-term tests described in a subsequent section of this report. It is reasonable to include a complete history of one such panel.

Panel No. 095, although not included in the long-term test program, was committed to an interesting test program. After a brief period of daily firing, with results tabulated in Table VIII, the individual pressure cells were paralleled and 1000 volts were applied to the paralleled cells. The panel was monitored continuously for erroneous firings for 107 days. Periodically, the applied voltage was increased until a firing event occurred, i.e., until one of the paralleled cells fired, and then lowered again to 1000 volts. During this test period no "failures" or erroneous firings occurred. The histogram of Fig. 17 shows the distribution of the 78 periodic firings. The average value of this distribution is 1162 volts. The medium value falls between 1150 volts and 1160 volts; the minimum is 1110 volts and the maximum is 1200 volts. If this distribution is divided into two halves according to time, the first-half average is 1160 volts with minimum and maximum values of 1110 and 1200 volts; and the second-half average is 1163 volts with a minimum and maximum values of 1120 and 1190 volts. These data show uniform panel characteristics that do not change with time. Four cells of Panel No. 092 were omitted from the tests described above and committed to other tests. One of these four initially fired at a voltage below 1000 volts.

Table VII

FIRING VOLTAGES FOR PANEL NO. 092

Cell No.	14.7 PSIA 4/26/71	p < 10 μHg 4/27/71	4/28/71	4/28/71	4/30/71	5/3/71	5/4/71	5/5/71	5/6/71
1	1410	1170	1180	1190	1180	1180	1170	1180	1180
2	1440	1230	1410	1280	1310	1320	1300	1330	1330
3	1370	1230	1270	1230	1240	1240	1260	1220	1260
4	1420	1260	1260	1260	1250	1240	1250	1320	1250
5	1480	1290	1300	1390	1300	1280	1320	1350	1350
6	1500	1260	1350	1230	1260	1270	1230	1300	1280
7	1400	1230	1320	1250	1280	1260	1290	1280	1290
8	1450	1320	1320	1320	1290	1280	1330	1300	1310
9	1540	1290	1320	1280	1270	1290	1290	1400	1330
10	1410	1220	1220	1150	1220	1220	1260	1230	1230
11	1510	1260	1230	1230	1230	1230	1250	1260	1240
12	1480	1280	1290	1270	1290	1280	1300	1300	1280
13	1440	1280	1280	1270	1280	1280	1290	1310	1240
14	1430	1190	1190	1190	1180	1190	1190	1190	1190
15	1390	1270	1280	1270	1220	1270	1320	1280	1300
16	1410	1230	1230	1250	1200	1210	1260	1240	1290
17	1450	1250	1260	1240	1220	1260	1290	1230	1260
18	1460	1200	1170	1200	1170	1210	1250	1220	1220

Table VII (Continued)

FIRING VOLTAGES FOR PANEL NO. 092

Cell No.	5/7/71	p < 10 μHg 5/10/71	5/11/71	14.7 PSIA 5/11/71	5/12/71	5/13/71	p < 10 μHg 5/14/71	5/17/71	5/19/71
1	1150	1200	1210	1420	1170	1180	1170	1150	1170
2	1290	1300	1270	1440	1240	1280	1310	1240	1270
3	1260	1280	1250	1400	1230	1230	1240	1230	1220
4	1250	1240	1250	1420	1220	1220	1220	1260	1250
5	1300	1300	1350	1460	1330	1340	1330	1290	1300
6	1320	1260	1270	1440	1230	1240	1270	1280	1290
7	1270	1240	1250	1410	1280	1220	1270	1270	1260
8	1280	1320	1310	1480	1310	1320	1320	1290	1280
9	1350	1330	1340	1470	1270	1280	1320	1300	1320
10	1210	1210	1210	1410	1190	1190	1190	1220	1220
11	1220	1230	1220	1420	1220	1220	1210	1200	1210
12	1290	1280	1280	1460	1270	1270	1270	1270	1270
13	1280	1270	1280	1420	1250	1230	1280	1260	1270
14	1170	1190	1350	1350	1180	1170	1200	1180	1180
15	1220	1280	1260	1410	1300	1240	1250	1280	1230
16	1220	1250	1240	1360	1240	1220	1220	1190	1220
17	1300	1220	1270	1460	1200	1230	1280	1250	1250
18	1190	1240	1180	1400	1180	1190	1220	1190	1240

Table VII (Continued)

FIRING VOLTAGES FOR PANEL NO. 092

Cell No.	5/20/71	14.7 PSIA 5/20/71	(In cold-vac. chamber) T ≃ 25°C 14.7 PSIA 6/10/71	p>45μHg 6/11/71	14.7 PSIA 7/9/71	7/15/71	T ≃ LN_2 10 μHg 9/14/71
1	1190	1400	1370	1170	1420	1370	1370
2	1270	1520	----	1210	1440	1380	1570
3	1210	1410	1350	1170	1380	1340	1540
4	1220	1420	----	1250	1430	1400	1690
5	1260	1490	1430	1240	1480	1480	1900
6	1280	1470	----	1220	1450	1370	1510
7	1220	1420	1410	1210	1440	1420	1550
8	1320	1420	----	1290	1460	1430	1580
9	1280	1470	1440	1260	1420	1450	1660
10	1210	1350	----	1240	1400	1360	1500
11	1200	1390	1360	1200	1450	1390	1540
12	1260	1450	----	1270	1450	1430	1560
13	1260	1390	1390	1260	1400	1420	1500
14	1180	1340	----	1170	1360	1370	1480
15	1210	1430	1430	1260	1470	1490	1500
16	1210	1370	----	1180	1390	1360	1400
17	1240	1420	1380	1180	1380	1380	1470
18	1200	1380	1340	1160	1350	1360	1480

TABLE VIII

FIRING VOLTAGES FOR PANEL NO. 095

Cell No.	5/21/71 p = 14.7 PSIA	5/24/71	5/25/71 Vacuum	5/26/71
1	1370	1160	1170	1160
2	1460	1310	1270	1280
3	1540	1340	1290	1230
4	1390	1280	1280	1260
5	1390	1240	1280	1280
6	1420	1200	1190	1130
7	1380	1180	1180	1160
8	1430	1270	1260	1240
9	1440	1270	1300	1290
10	1160	970	940	940
11	1490	1340	1340	1330
12	1430	1250	1220	1270
13	1470	1300	1290	1270
14	1440	1270	1220	1220
15	1430	1280	1280	1320
16	1440	1270	1270	1260
17	1410	1220	1240	1220
18	1390	1180	1210	1230

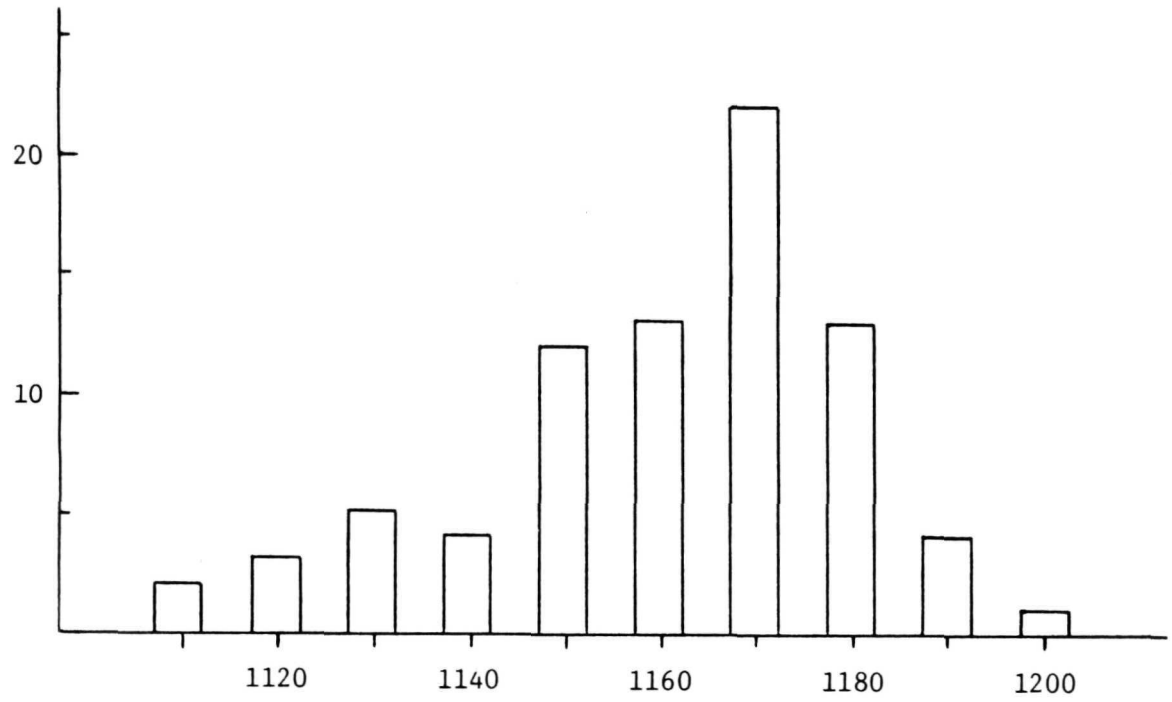

Fig. 17. Histogram Showing Minimum Firing Voltage of Panel No. 095.

Three other panels were similarly tested but for a lesser period of time. Panel No. 084 was energized at 800 volts for a period of 90 days, No. 114 at 800 volts for a period of 33 days and No. 154 at 1000 volts for a period of 10 days. Daily firings yielded uniform results and no failures occurred. These tests were terminated to facilitate routine and long-term tests of additional panels.

SECTION IV

LONG-TERM EXPERIMENT

Description of the Experiment

As flight quality panels were received for long-term testing, they were routinely tested as follows. Leakage impedances of the individual cells were checked at 1000 volts and determined to be greater than 10^{13} Ω. The individual cells were fired in an ambient pressure of 14.7 PSIA, then placed in a vacuum at room temperature and fired on several occasions over a period of several days. Some panels, e.g., Panel No. 092, received extensive testing prior to the beginning of the long-term test. Additionally, panels committed to testing in a cold vacuum were tested after being wired in the cold-vacuum test facility. They were fired at room temperature and 14.7 PSIA, at room temperature in a vacuum, cooled to near liquid nitrogen temperature and fired, and warmed to room temperature and fired. All of the long-term test panels were fired periodically prior to beginning the scheduled, long-term test program. All of these tests yielded the anticipated results, i.e., no erroneous firings and satisfactory firing voltages when the cells were forced to fire by increasing the applied voltage.

As the long-term test began, the panels in the cold vacuum facility were cycled to room temperature again after a period of two weeks near liquid nitrogen temperature, fired at room temperature, and cooled again for the duration of the experiment. All results were as expected. Voltages did not change significantly and no failures were observed. It is observed that firing voltages at liquid nitrogen temperature increased slightly over room temperature voltages.

Panels were committed to the long-term tests as follows. Panels No. 137, 146, 151 and 161 were placed in a vacuum bell-jar and maintained in a vacuum at room temperature. Panels No. 092, 114, 125 and 154 were placed in a cold-vacuum facility and maintained in a vacuum near liquid nitrogen (LN_2) temperature (-195°C). (The panel numbers are serial numbers assigned at LRC during fabrication and are traceable through the fabrication process.) Criteria applied to this selection include fabrication according to MDE specifications and satisfactory results during preliminary testing. Additionally, panels selected for the cold-vacuum conditions included those most extensively tested at room temperature.

Pressure cells mounted in each of the two test facilities, i.e., room temperature-vacuum and cold-vacuum, were committed to one of six groups for subsequent testing, i.e., weekly, monthly, quarterly, semi-annual,

annual and unscheduled groups. The weekly group cells were fired on a weekly basis, the monthly group on a monthly basis, etc. The unscheduled group was eventually fired with the annual group. Pressure cell assignments within the six groups are tabulated in Table IX. This arrangement distributes each group of cells that are fired together throughout the panels and locations within a panel.

Table IX
Pressure Cell Firing Schedule

Panel No.	Periods* 1	4	12	24	48	Unscheduled
092	1, 2, 10	3, 11, 12	4, 6, 13	7, 14, 15	8, 9, 16	17, 18
114	3, 11, 12	4, 5, 13	6, 14, 15	7, 8, 16	9, 17, 18	2, 10
125	4, 5, 13	6, 14, 15	7, 8, 16	9, 18, 10	1, 2, 11	3, 12
154	6, 14, 15	7, 8, 16	9, 17, 18	1, 2, 10	3, 11, 12	4, 5, 13
137	2, 3, 10	4, 11, 12	5, 6, 13	7, 14, 15	8, 9, 16	17, 18
146	5, 11, 12	6, 7, 13	8, 14, 15	1, 2, 16	3, 17, 18	10
151	5, 8, 13	9, 14, 15	1, 2, 16	3, 17, 18	4, 10, 11	12
161	9, 14, 15	10, 11, 16	1, 17, 18	2, 3, 12	4, 5, 8	6, 7, 13

*A period is 1 week.

Circuitry Description - Figure 18 is a block diagram of the long-term test circuitry. The primary power source supplies power to the test circuitry through a standby power unit which, in the event of a power failure, can continue to supply the experiment from a battery pack. The standby unit keeps the battery pack in a fully-charged condition by a taper-charge cycle whenever battery voltage decreases. Time constants of the power supply output filters are such that transients due to a switchover from primary to battery source and back are negligible. For example, voltage transients from the high voltage power supply are less than 0.05 volts when the primary power supply is switched ON or OFF. The test circuitry illustrated in Fig. 18 basically utilizes the MDE transducer circuitry. This circuitry is illustrated in Fig. 19. Energy to fire a transducer is stored on the associated .01 μf capacitor which discharges through the transducer, the 2.2 kΩ and 10^5 Ω resistors during a firing event. The firing event is detected across the 2.2 kΩ resistor. The 10^7 Ω resistor limits current to a firing transducer and, consequently, it ceases to conduct after the capacitor dischages. Each supply circuit and each flip flop monitors 12 paralleled transducers, as illustrated in Fig. 19. The capacitor

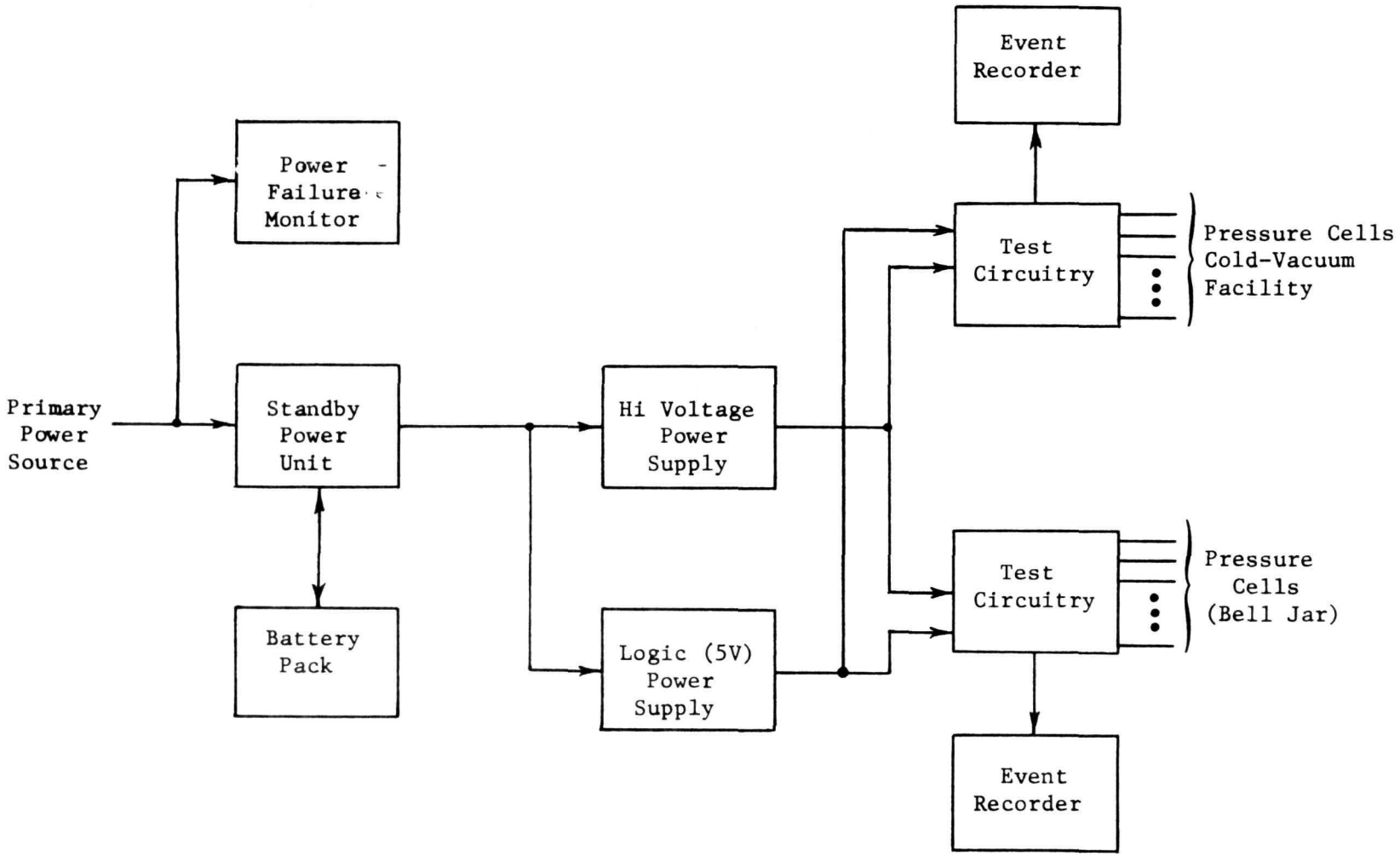

Fig. 18. Long-Term Test Electronic Apparatus

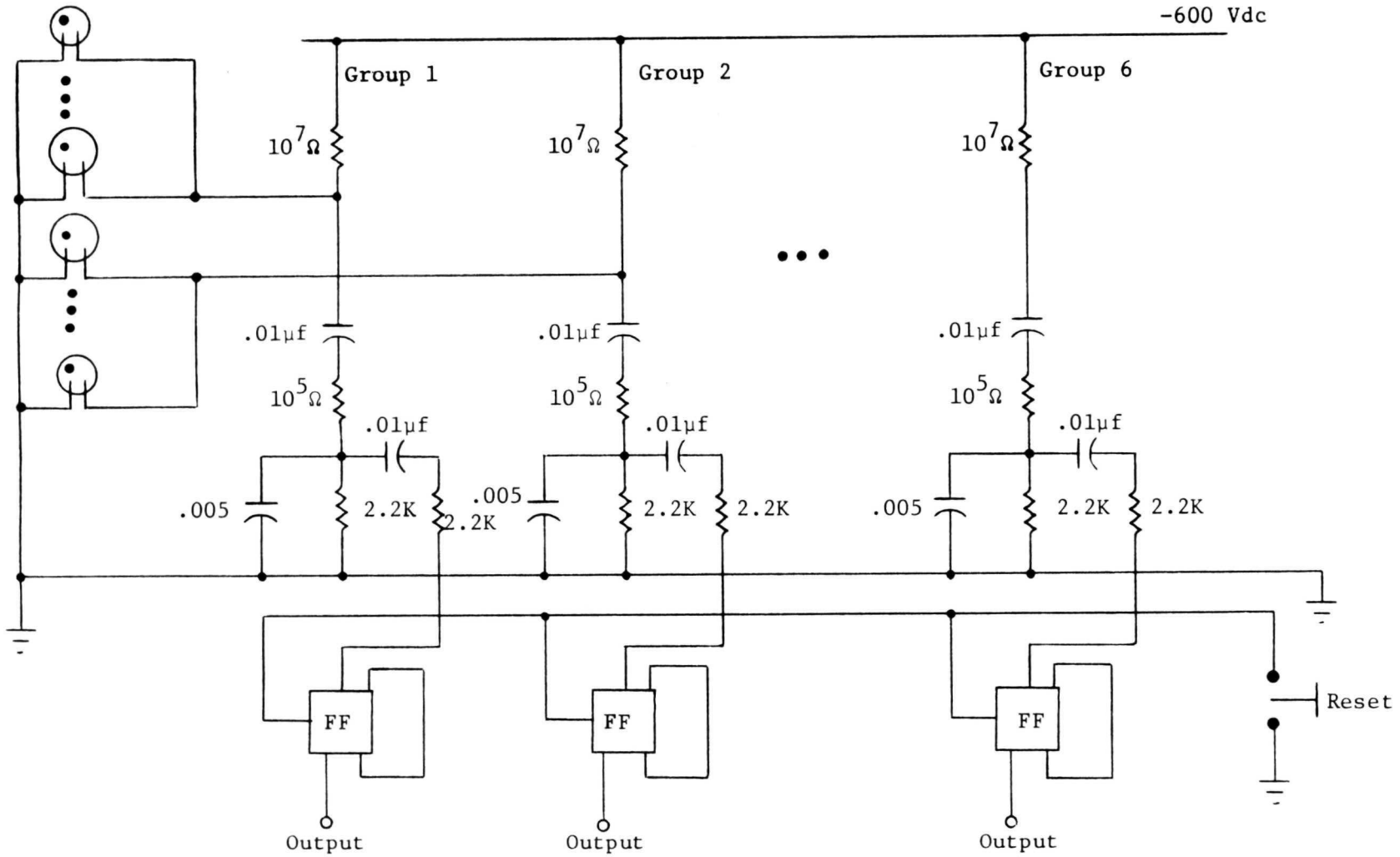

Fig. 19. Long-Term Test Circuitry

recharges through the $10^7\Omega$ resistor. This portion of the transducer circuitry has been described previously and will not be discussed further here [Ref. 1]. The output across the 2.2 kΩ resistor is coupled to an associated flip flop which is configured to latch-up whenever a transducer fires. The coupling circuitry parameter values were determined experimentally and selected to assure that a firing event would be recorded by the associated flip flop only and no others. (Physical and thermal considerations necessitated long, parallel runs of wires to transducers in separate groups.) A separate chassis housing the circuitry illustrated in Fig. 19 was used for each of the two test facilities. Different types of flip flops were used in the two chassis and the coupling circuitry differed slightly between the two.

Additional details of the monitoring circuitry are illustrated in Fig. 20. Each of the 12 monitor circuit segments was connected to its group of 12 associated transducers (pressure cells) through the switching arrangement illustrated. (Two rotary switches were required for each segment, as illustrated.) The switches are shown in the MONITOR position, and every transducer is supplied from the -600 Vdc supply through the monitoring circuit. If any of the twelve transducers fired, the flip flop in the monitoring circuit would latch-up illuminating the LED. When a group was to be fired, the group selector switch and the cell selector switch were positioned to select a single transducer for testing. The selected transducer was supplied from a separate monitor circuit and power supply, and the power supply voltage was increased in decade steps until the transducer fired. All other transducers continued to be supplied and monitored routinely. (All switch contacts other than the selected contact are connected together.) The test circuitry ouput had a larger amplitude because of the $10^4\Omega$ output resistor and was used to drive a recorder. The circuitry illustrated in Fig. 20 was arranged in two chassis consisting of six segments each. Each chassis monitored the six groups in either the cold-vacuum facility or the room temperature facility.

The switching circuitry illustrated in Fig. 20 also provided a capability of routinely monitoring a single transducer, i.e., the variable high voltage could be set at -600 V and switched to any transducer. A faulty transducer could possibly have been isolated in this fashion.

Figure 21 is a photograph of one of the circuitry chassis described above. In Fig. 22, the back of the chassis is opened to show the switching and monitoring circuitry.

Vacuum Apparatus Description - The vacuum apparatus used for the long-term test is illustrated in Fig. 23. The test panels were continuously in a vacuum; one group of four panels at room temperature and a second group of four near liquid nitrogen temperature (-195°C). The vacuum in each test facility was monitored by a thermocouple gauge, and a thermocouple was used to monitor temperature in the cold-vacuum facility. The two pressure

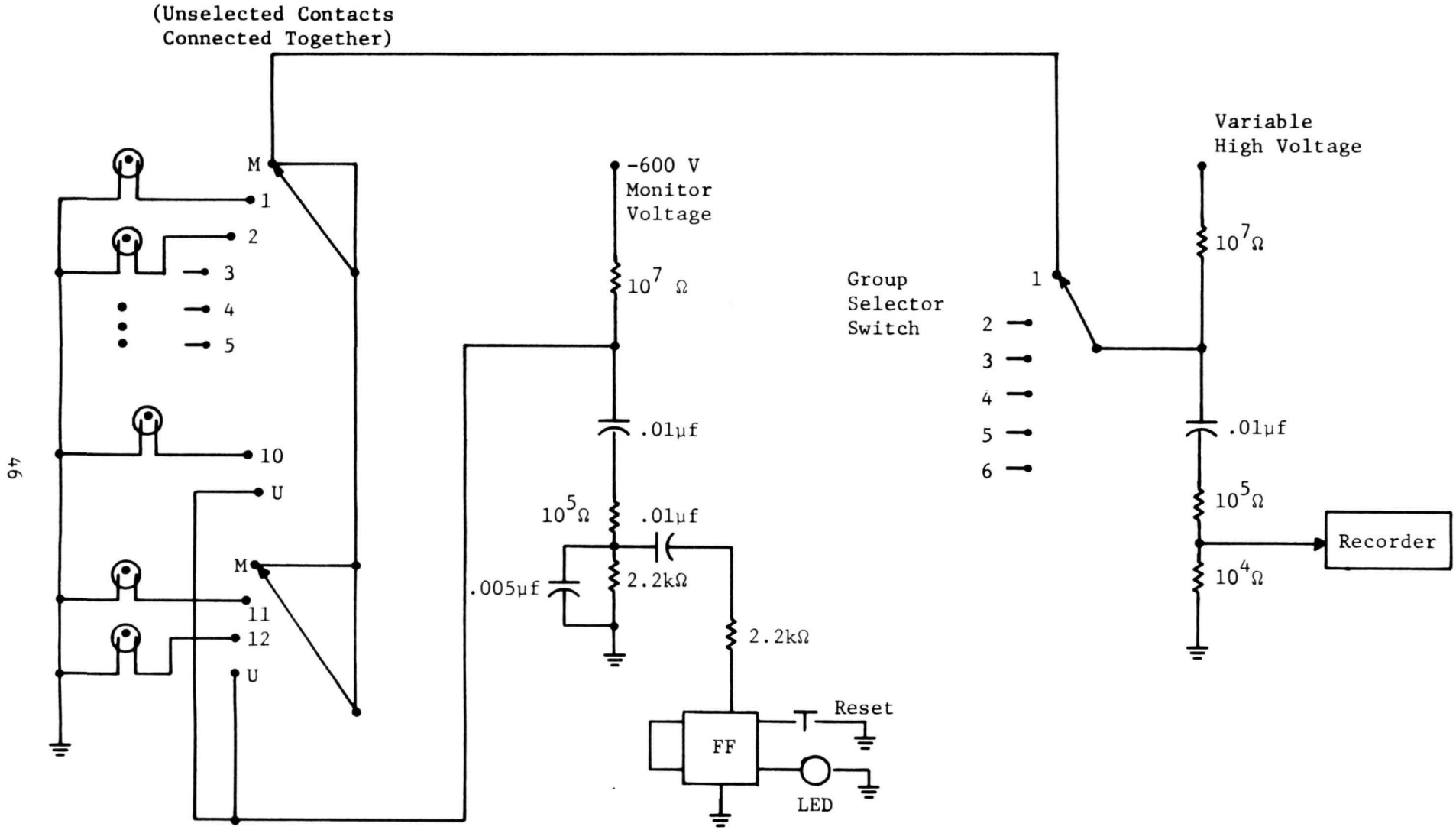

Fig. 20. Long-Term Test Monitoring Circuit (one segment)

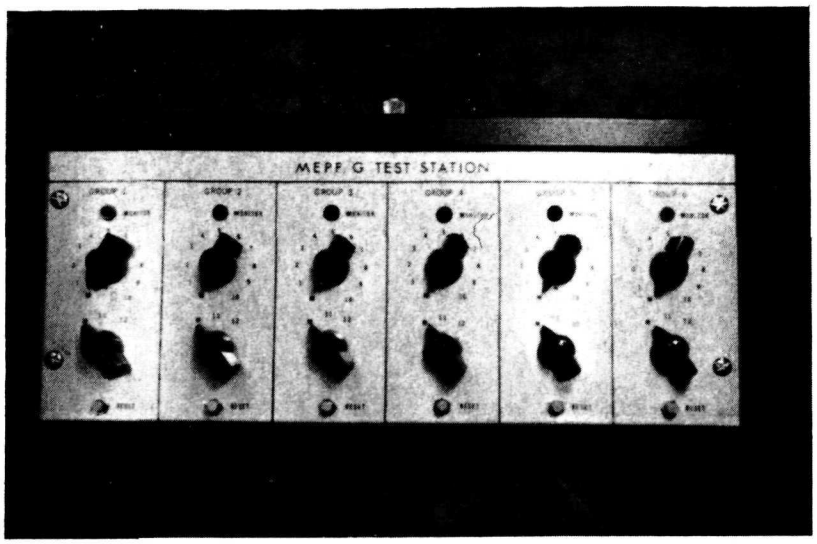

Fig. 21. Photograph of Monitoring Circuit Chassis

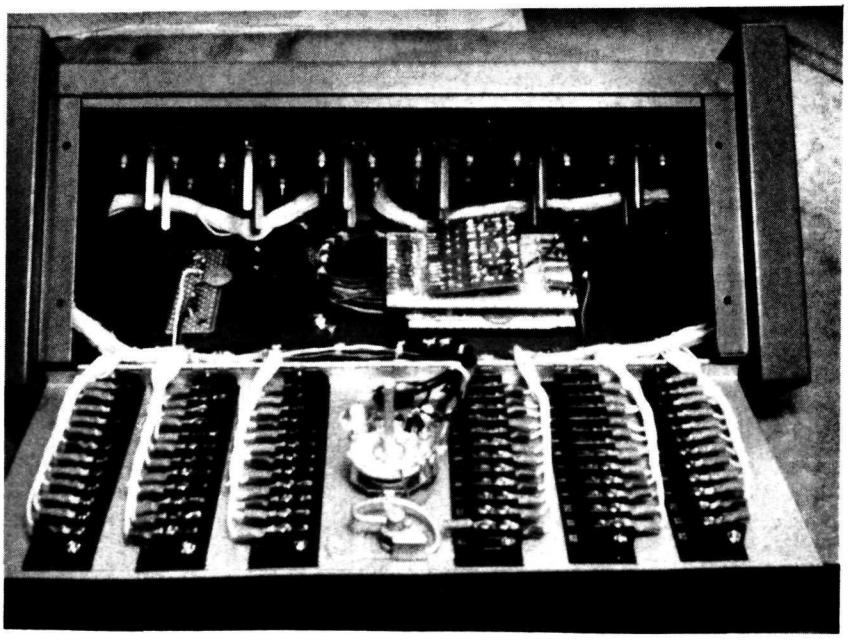

Fig. 22. Interior View of Monitoring Circuit Chassis

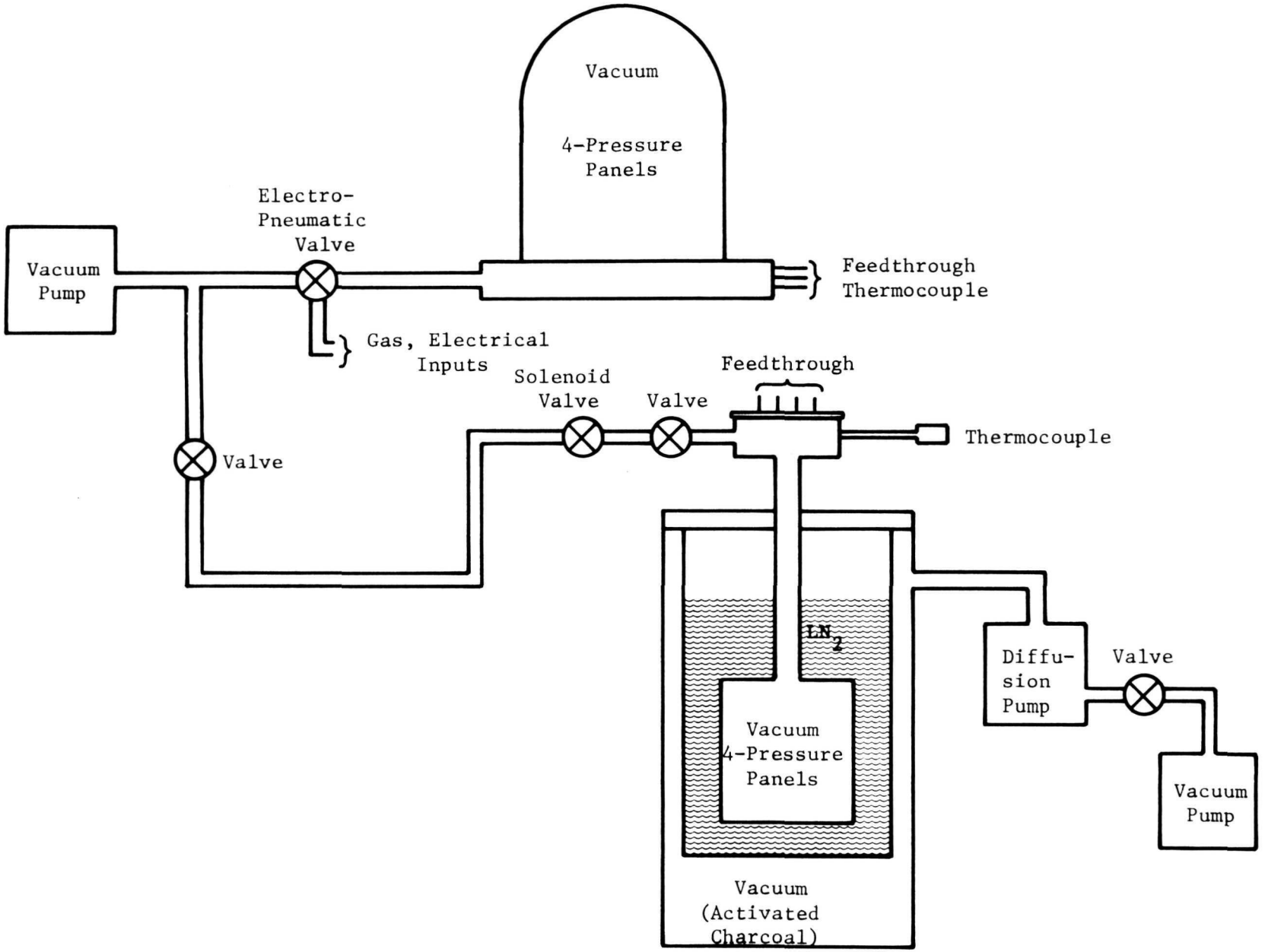

Fig. 23. Vacuum Apparatus

chambers were isolated in the event of a power failure by the electro-pneumatic valve illustrated in Fig. 23. The cold-vacuum facility was a large-mouthed cryostat fabricated of stainless steel. The outer chamber was continuously pumped to maintain an insulating vacuum. An adequate level of LN_2 was maintained throughout the entire period of the experiment by periodic refills.

Figure 24 is a photograph of the long-term experiment apparatus. The cold-vacuum facility is located on the right, and the room temperature, bell jar facility is on the left. The electronics is located on the bench to the left of the bell jar, and power supplies and vacuum monitors are located behind and on the shelves above the bell jar. Figure 25 is a close-up of the upper portion of the cold-vacuum facility.

Facility Monitoring Procedures - Pressure in the two vacuum facilities was continuously monitored by thermocouple gauges. Additionally, a measure of the pressure in the cold vacuum facility was determined by routinely firing a pair of electrodes, i.e., an unmounted transducer, located inside the facility. The firing voltage of this transducer was routinely above 2,000 volts; however, it was observed to steadily decrease concurrently with an increasing pressure in the cold-vacuum chamber. The decrease occurred over a period of approximately one month to a firing voltage of 1,500 volts. The cold-vacuum chamber pressure during this period increased from a near zero (<1 μHg) reading on a thermocouple gauge to 40 μHg. After the vacuum pump was serviced, the unmounted transducer firing voltage again exceeded 2,000 volts and the thermocouple gauge indicated near zero pressure. At the termination of the long-term test, the unmounted transducer was fired periodically as the cold-vacuum chamber pressure slowly increased. At 20 μHg, the firing voltage was 1,570 volts, and at 40 μHg it was 1,400 volts. These values are in reasonable agreement with the pressure and firing voltage values observed during the tests.

Experimental Results, A Summary

The eight pressure panels committed to the long-term experiment were monitored continuously for erroneous firings and fired periodically according to schedule. The results of these firings are summarized in this section. A tabulation of all firing events is included in this report as Appendix A.

Tables X through XVII summarize the firing results from the eight long-term test panels. Each table summarizes data from a single panel. (Cells for which no data are recorded were not included in the experiment for various reasons.) Tables X through XIII summarize results from the panels tested at LN_2 temperature. Tabulated for each cell are averaged values of firing voltages at room temperature--atmospheric pressure and room temperatures--vacuum pressure prior to the long term test, long-

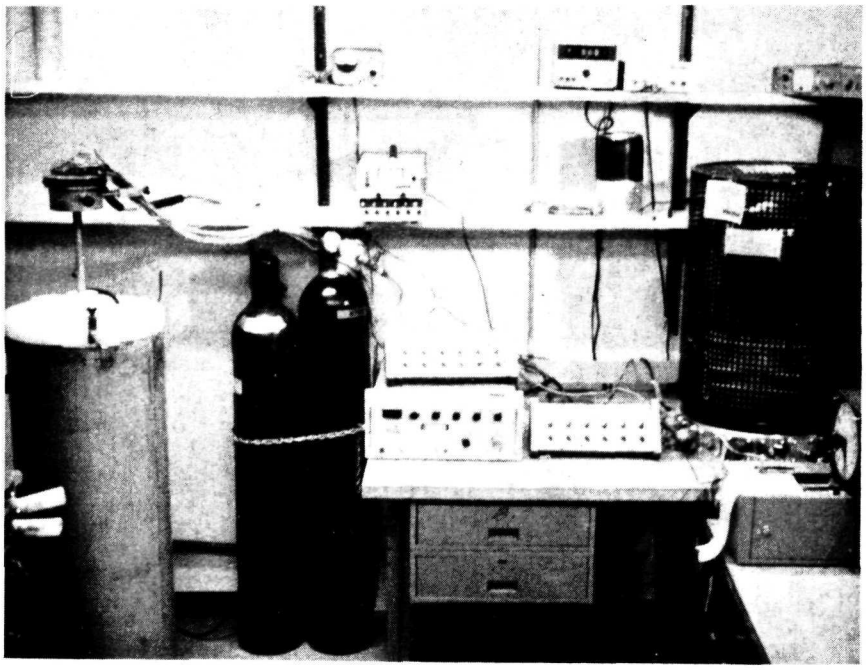

Fig. 24. Photograph of the Long-Term Test Apparatus

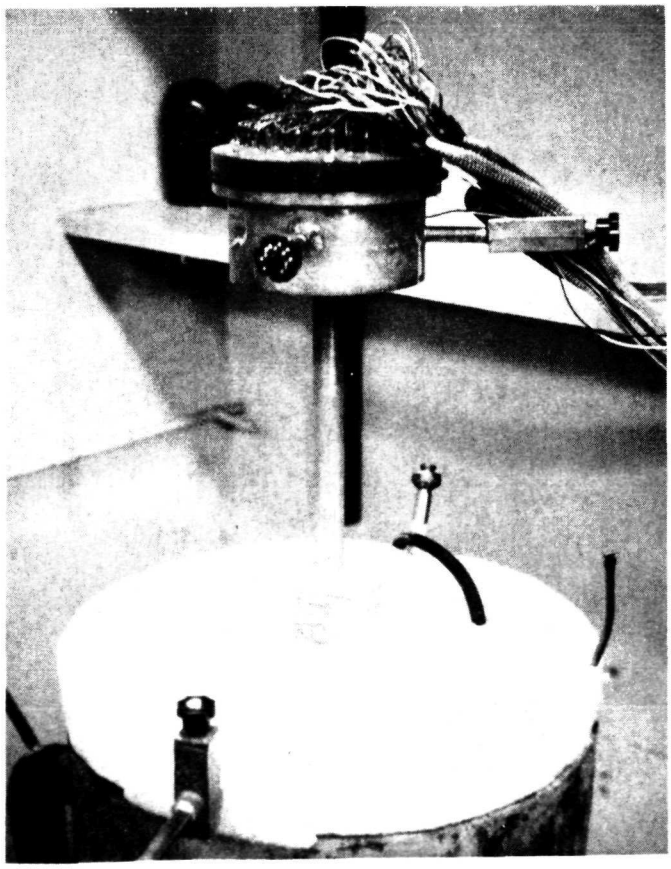

Fig. 25. Close-up View of the Cold-Vacuum Facility

TABLE X
SUMMARY OF FIRING RESULTS, PANEL NO. 092 (LN_2 Temperature)

Panel, Cell No.		Rm. Temp., Atmos. Avg. Volts	No. Samples	Rm. Temp., Vac. Avg. Volts	No. Samples	Long-Term Test Avg. Volts	No. Samples	Rm. Temp. Vac. Avg. Volts	No. Samples	Rm. Temp. Atmos. Avg. Volts	No. Samples
092	1	1340	1	1187	3	1392	48	1140	3	1330	2
	2	1390	1	1213	3	1526	48	1180	3	1385	2
	3	1340	1	1200	3	1446	14	1187	3	1380	2
	4	1380	1	1243	3	1430	6	1213	3	1375	2
	5										
	6	1400	1	1217	3	1392	6	1180	3	1360	2
	7	1410	1	1233	3	1468	4	1270	3	1400	2
	8	1450	1	1287	3	1497	3	1270	3	1405	2
	9	1450	1	1240	3	1497	3	1233	3	1420	2
	10	1390	1	1190	3	1479	48	1186	3	1365	2
	11	1390	1	1217	3	1466	14	1213	3	1380	2
	12	1430	1	1213	3	1497	14	1253	3	1410	2
	13	1400	1	1210	3	1440	6	1207	3	1360	2
	14	1320	1	1183	3	1394	4	1177	3	1325	2
	15	1370	1	1243	3	1475	4	1253	3	1365	2
	16	1360	1	1195	2	1450	3	1220	3	1365	2
	17	1380	1	1203	3	1507	3	1203	3	1375	2
	18	1330	1	1157	3	1373	3	1170	3	1330	2

TABLE XI
SUMMARY OF FIRING RESULTS, PANEL NO. 114 (LN_2 Temperature)

Panel, Cell No.		Rm. Temp., Atmos. Avg. Volts	Rm. Temp., Atmos. No. Samples	Rm. Temp., Vac. Avg. Volts	Rm. Temp., Vac. No. Samples	Long-Term Test Avg. Volts	Long-Term Test No. Samples	Rm. Temp. Vac. Avg. Volts	Rm. Temp. Vac. No. Samples	Rm. Temp. Atmos. Avg. Volts	Rm. Temp. Atmos. No. Samples
114	1										
	2	1610	1	1435	2	1777	3	1383	3	1570	2
	3	1640	1	1500	2	1705	48	1403	3	1335	2
	4	1590	1	1445	2	1728	14	1437	3	1575	2
	5	1560	1	1420	2	1745	14	1407	3	1550	2
	6	1530	1	1400	2	1665	6	1403	3	1560	2
	7	1660	1	1495	2	1728	4	1490	3	1575	2
	8	1570	1	1395	2	1723	4	1360	3	1545	2
	9	1690	1	1520	2	1907	3	1510	3	1705	2
	10	1650	1	1405	2	1693	3	1370	3	1600	2
	11	1600	1	1350	2						
	12	1670	1	1475	2	1771	48	1507	3	1660	2
	13	1660	1	1475	2	1766	14	1433	3	1650	2
	14	1550	1	1390	2	1638	6	1330	3	1540	2
	15	1730	1	1530	2	1742	6	1503	3	1690	2
	16	1450	1	1325	2	1623	4	1303	3	1470	2
	17	1630	1	1335	2	1650	3	1393	3	1525	2
	18	1710	1	1490	2	1333	3	1447	3	1660	2

TABLE XII
SUMMARY OF FIRING RESULTS, PANEL NO. 125 (LN_2 Temperature)

Panel, Cell No	Rm. Temp., Atmos. Avg. Volts	No. Samples	Rm. Temp., Vac. Avg. Volts	No. Samples	Long-Term Test Avg. Volts	No. Samples	Rm. Temp. Vac. Avg. Volts	No. Samples	Rm. Temp. Atmos. Avg. Volts	No. Samples
125 1	1440	1	1200	2	1383	3	1210	3	1410	2
2	1320	1	1135	2	1377	3	1143	3	1295	2
3	1400	1	1135	2	1360	3	1130	3	1265	2
4	1330	1	1135	2	1465	48	1160	3	1300	2
5	1430	1	1165	2	1437	48	1223	3	1390	2
6	1500	1	1255	2	1456	14	1260	3	1450	2
7	1440	1	1140	2	1417	6	1137	3	1375	2
8	1410	1	1170	2	1437	6	1190	3	1360	2
9	1400	1	1145	2	1370	4	1143	3	1430	2
10	1370	1	1185	2	1393	4	1207	3	1350	2
11	1410	1	1195	2	1433	3	1237	3	1370	2
12	1400	1	1145	2	1403	3	1157	3	1240	2
13	1370	1	1205	2	1453	48	1223	3	1360	2
14	1320	1	1155	2	1378	14	1150	3	1265	2
15	1400	1	1145	2	1401	14	1197	3	1335	2
16	1470	1	1220	2	1420	6	1207	3	1345	2
17										
18	1440	1	1155	2	1358	4	1177	3	1350	2

TABLE XIII
SUMMARY OF FIRING RESULTS, PANEL NO. 154 (LN_2 Temperature)

Panel, Cell No.		Rm. Temp., Atmos. Avg. Volts	No. Samples	Rm. Temp., Vac. Avg. Volts	No. Samples	Long-Term Test Avg. Volts	No. Samples	Rm. Temp. Vac. Avg. Volts	No. Samples	Rm. Temp. Atmos. Avg. Volts	No. Samples
154	1	1530	1	1265	2	1440	4	1297	3	1420	2
	2	1490	1	1275	2	1503	4	1263	3	1420	2
	3	1540	1	1355	2	1520	3	1353	3	1520	2
	4	1440	1	1330	2	1437	3	1320	3	1480	2
	5	1550	1	1345	2	1493	3	1347	3	1470	2
	6	1570	1	1340	2	1488	48	1357	3	1450	2
	7	1470	1	1320	2	1505	14	1337	3	1460	2
	8	1630	1	1420	2	1609	14	1437	3	1590	2
	9	1670	1	1415	2	1525	6	1440	3	1600	2
	10	1460	1	1295	2	1445	4	1280	3	1435	2
	11	1520	1	1310	2	1500	3	1317	3	1470	2
	12	1460	1	1290	2	1433	3	1297	3	1445	2
	13	1440	1	1260	2	1440	3	1270	3	1390	2
	14	1520	1	1325	2	1513	48	1303	3	1445	2
	15	1490	1	1405	2	1474	48	1330	3	1415	2
	16	1460	1	1320	2	1492	14	1317	3	1465	2
	17	1540	1	1345	2	1508	6	1327	3	1485	2
	18	1420	1	1230	2	1403	6	1217	3	1425	2

TABLE XIV
SUMMARY OF FIRING RESULTS, PANEL NO. 137 (Room Temperature)

Panel, Cell No.	Rm. Temp., Atmos. Avg. Volts	Rm. Temp., Atmos. No. Samples	Rm. Temp., Vac. Avg. Volts	Rm. Temp., Vac. No. Samples	Long Term Test Avg. Volts	Long Term Test No. Samples	Rm. Temp. Atmos. Avg. Volts	Rm. Temp. Atmos. No. Samples
137 1								
2	1540	1	1310	2	1319	49	1385	2
3	1560	1	1305	2	1279	49	1455	2
4	1400	1	1260	2	1334	14	1350	2
5	1390	1	1170	2	1155	6	1290	2
6	1490	1	1320	2	1265	6	1460	2
7	1500	1	1300	2	1275	4	1460	2
8	1470	1	1275	2	1240	3	1375	2
9	1420	1	1305	2	1300	3	1470	2
10	1430	1	1360	2	1269	48	1425	2
11	1480	1	1335	2	1320	14	1450	2
12	1420	1	1265	2	1272	14	1395	2
13	1440	1	1270	2	1273	6	1415	2
14	1430	1	1265	2	1258	4	1410	2
15	1420	1	1295	2	1265	4	1420	2
16	1410	1	1200	2	1197	3	1355	2
17	1480	1	1310	2	1273	3	1465	2
18	1400	1	1590	2	1577	3	1670	2

TABLE XV
SUMMARY OF FIRING RESULTS, PANEL NO. 146 (Room Temperature)

Panel, Cell No.		Rm. Temp., Atmos.		Rm. Temp., Vac.		Long Term Test		Rm. Temp., Atmos.	
		Avg. Volts	No. Samples	Avg. Volts	No. Samples	Avg. Volts	No. Samples	Avg. Volts	No. Samples
146	1	1750	1	1450	2	1448	4	1670	2
	2	1500	1	1270	2	1253	4	1460	2
	3	1540	1	1290	2	1260	3	1480	2
	4								
	5	1440	1	1235	2	1209	48	1380	2
	6	1460	1	1235	2	1236	14	1435	2
	7	1400	1	1205	2	1190	14	1375	2
	8	1410	1	1195	2	1185	6	1355	2
	9								
	10	1470	1	1275	2	1260	3	1415	2
	11	1420	1	1265	2	1215	48	1395	2
	12	1420	1	1240	2	1238	48	1395	2
	13	1410	1	1155	2	1141	14	1290	2
	14	1400	1	1190	2	1185	6	1340	2
	15	1400	1	1170	2	1207	6	1370	2
	16	1410	1	1200	2	1205	4	1365	2
	17	1390	1	1195	2	1137	3	1340	2
	18	1430	1	1170	2	1117	3	1350	2

TABLE XVI
SUMMARY OF FIRING RESULTS, PANEL NO. 151 (Room Temperature)

Panel, Cell No.		Rm. Temp., Atmos. Avg. Volts	Rm. Temp., Atmos. No. Samples	Rm. Temp., Vac. Avg. Volts	Rm. Temp., Vac. No. Samples	Long Term Test Avg. Volts	Long Term Test No. Samples	Rm. Temp. Atmos. Avg. Volts	Rm. Temp. Atmos. No. Samples
151	1	1370	1	1180	2	1178	6	1350	2
	2	1480	1	1155	2	1245	6	1445	2
	3	1460	1	1220	2	1205	4	1370	2
	4	1380	1	1230	2	1157	3	1315	2
	5	1380	1	1165	2	1151	48	1320	2
	6								
	7								
	8	1440	1	1210	2	1204	48	1390	2
	9	1350	1	1115	2	1162	14	1305	2
	10	1470	1	1275	2	1213	3	1395	2
	11	1460	1	1300	2	1237	3	1420	2
	12	1340	1	1215	2	1220	3	1390	2
	13	1300	1	1140	2	1136	48	1305	2
	14	1370	1	1160	2	1159	14	1305	2
	15	1400	1	1165	2	1168	14	1355	2
	16	1480	1	1255	2	1242	6	1400	2
	17	1430	1	1220	2	1188	4	1345	2
	18	1410	1	1135	2	1125	4	1315	2

TABLE XVII
SUMMARY OF FIRING RESULTS, PANEL NO. 161 (Room Temperature)

Panel, Cell No.		Rm. Temp., Atmos.		Rm. Temp., Vac.		Long Term Test		Rm. Temp., Atmos.	
		Avg. Volts	No. Samples	Avg. Volts	No. Samples	Avg. Volts	No. Samples	Avg. Volts	No. Samples
161	1	1560	1	1235	2	1237	6	1470	2
	2	1800	1	1430	2	1330	4	1485	2
	3	1570	1	1320	2	1270	4	1395	2
	4	1590	1	1255	2	1303	3	1455	2
	5	1530	1	1305	2	1260	3	1450	2
	6	1540	1	1300	2	1283	3	1460	2
	7	1580	1	1365	2	1350	3	1520	2
	8	1610	1	1365	2	1287	3	1455	2
	9	1630	1	1360	2	1344	48	1545	2
	10	1810	1	1365	2	1409	14	1600	2
	11	1620	1	1380	2	1368	14	1555	2
	12	1530	1	1320	2	1298	4	1435	2
	13	1610	1	1330	2	1343	3	1500	2
	14	1580	1	1365	2	1331	48	1460	2
	15	1570	1	1370	2	1360	48	1485	2
	16	1560	1	1340	2	1306	14	1565	2
	17	1640	1	1335	2	1270	6	1495	2
	18	1640	1	1320	2	1322	6	1480	2

term test averages, room temperature--vacuum pressure and room temperatures--atmospheric pressure after the long term test. The number of samples included in each average is also tabulated since it varies significantly from cell to cell. (The weekly results yield more data than monthly results, for example.) These tabulations show the effects of immersing the cells in a vacuum pressure and the effects of the cold temperature. As results with the experimental panels indicated, immersing the cells in a vacuum lowers the firing voltage (the cells expand, reducing gas density) and the low temperature increases the firing voltages. The significant observations are that the voltages remain at a reasonably uniform and satisfactory level for all conditions, and are reasonably repeatable after a year of testing. The uniformity of results obtained before and after the long-term experiment is excellent.

Tables XIV through XVII are comparable tabulations for the room temperature test panels. (Since the long-term tests for these panels correspond to room temperature--vacuum pressure, these tables require one less column.) The preceding discussion of the cold-vacuum test results applies equally well to these panels and the results are equally gratifying.

Variations in period to period firing voltages are illustrated by example in Fig. 26. The cells selected (Panel 092, Cells 2 and 10) are from the LN_2, weekly group because more data are available and the LN_2 firing voltages tend to be less uniform from period to period. These results show significant but acceptable variations in firing voltages throughout the long-term experiment. The variations appear to be random and not significantly correlated from cell to cell. The data tabulated in Appendix A tend to support these observations.

A similar plot is presented in Fig. 27 for two cells from the weekly room temperature group. These results are significantly more uniform.

Cell firing voltages from the weekly, monthly and quarterly groups were plotted on probability graph paper, and these plots were examined for any obvious data distributions. A few distributions appeared reasonably normal; however, most of the plots did not indicate anything other than a random distribution.

The most significant results from the long-term experiment are that the pressure cell firing voltages remained at a satisfactory value throughout the experiment and, with one exception which will be discussed in a subsequent section, no extraneous firing events occurred. Furthermore, when the experiment was terminated, all of the pressure cells were found to be in excellent condition. None had leaked or deteriorated in any observable way during the long-term experiment.

Figure 28 is a photograph of the room temperature, long-term test panels after the experiment was terminated and the bell jar removed. Figure 29 shows the inner chamber of the cold-vacuum facility with the

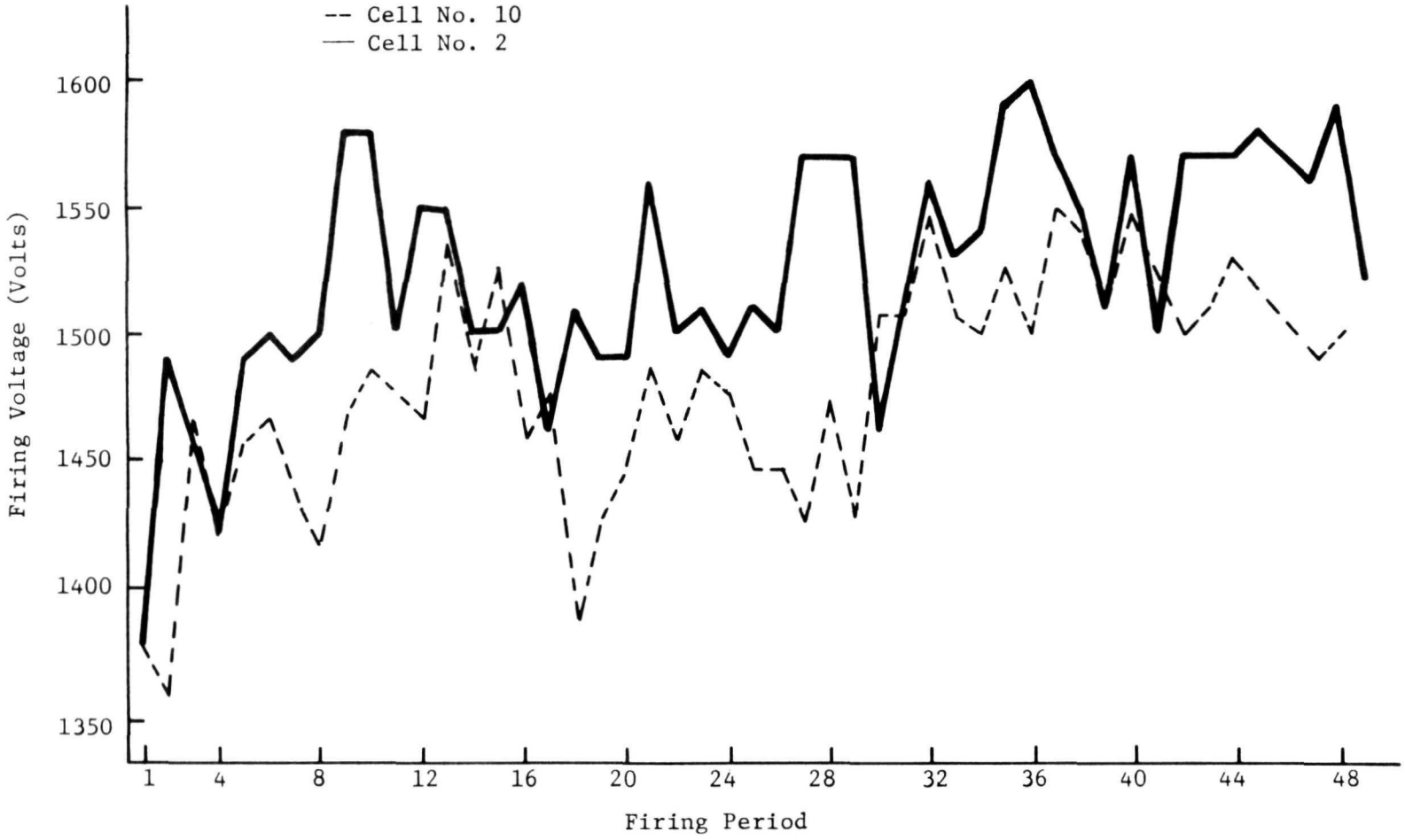

Fig. 26. Weekly, LN_2 Temperature Firing Voltages; Panel 092, Cells 2 and 10

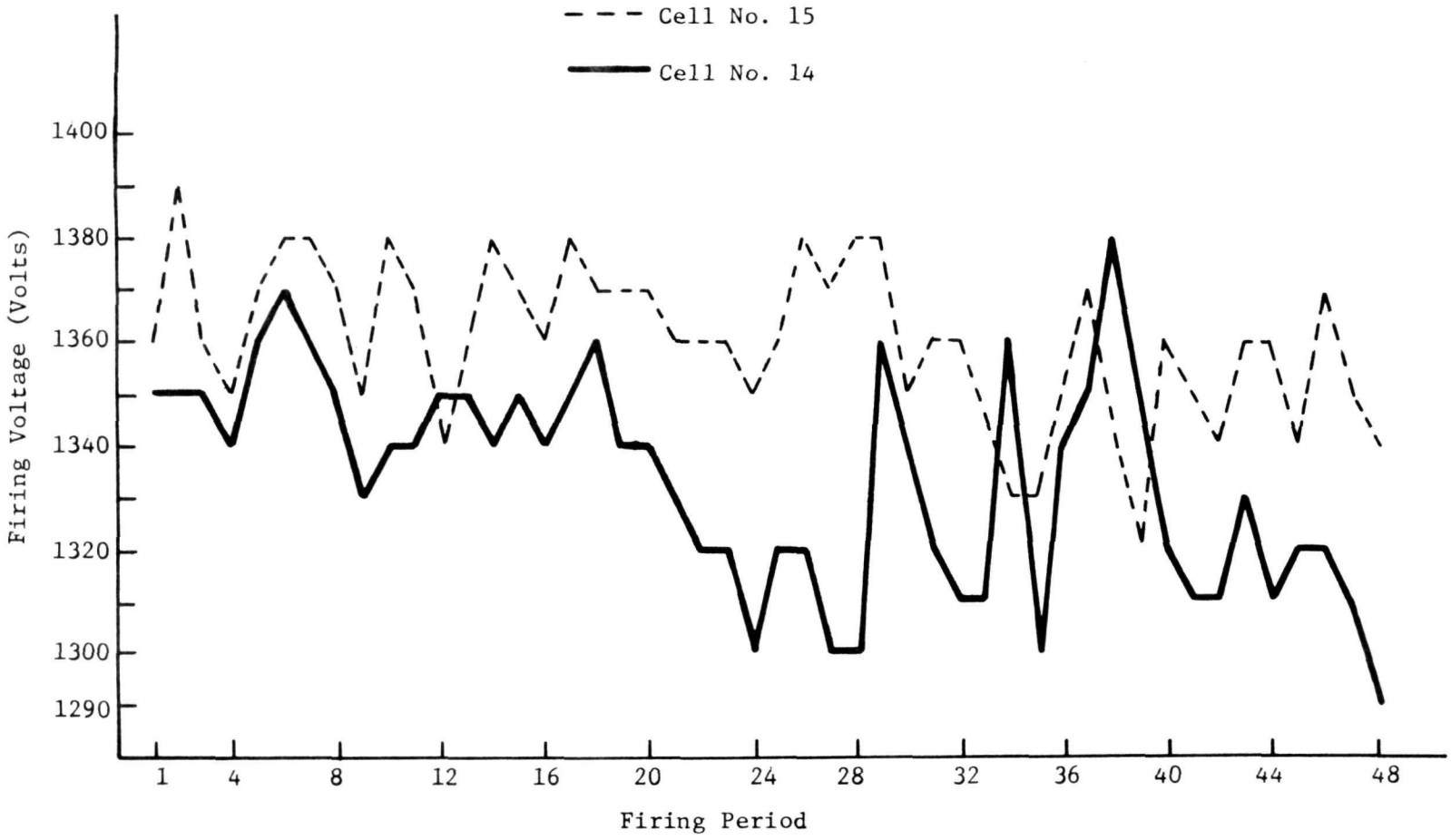

Fig. 27. Weekly, Room Temperature Firing Voltages; Panel 116, Cells 14 and 15

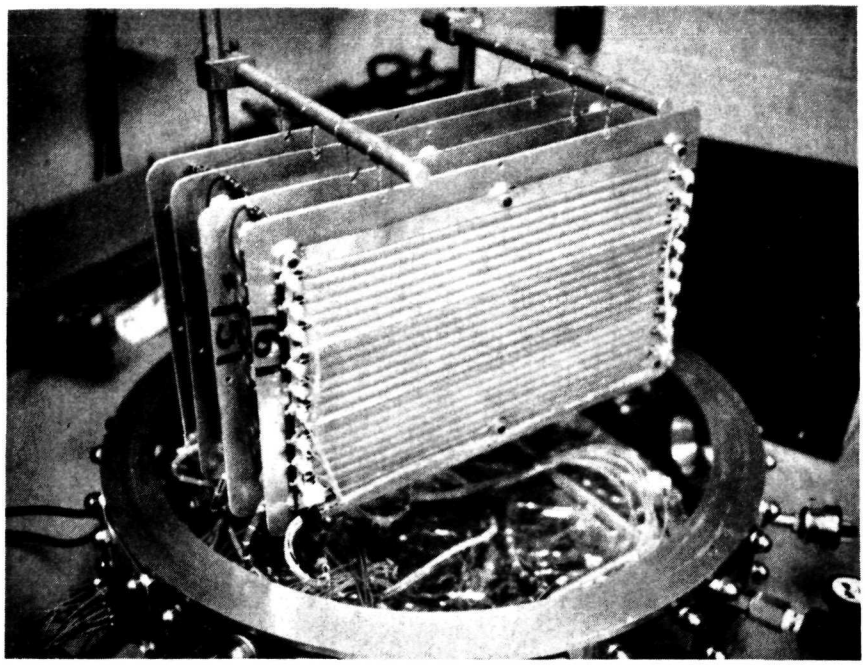

Fig. 28. Photograph of Room Temperature Test Panels After Completion of Long-Term Test

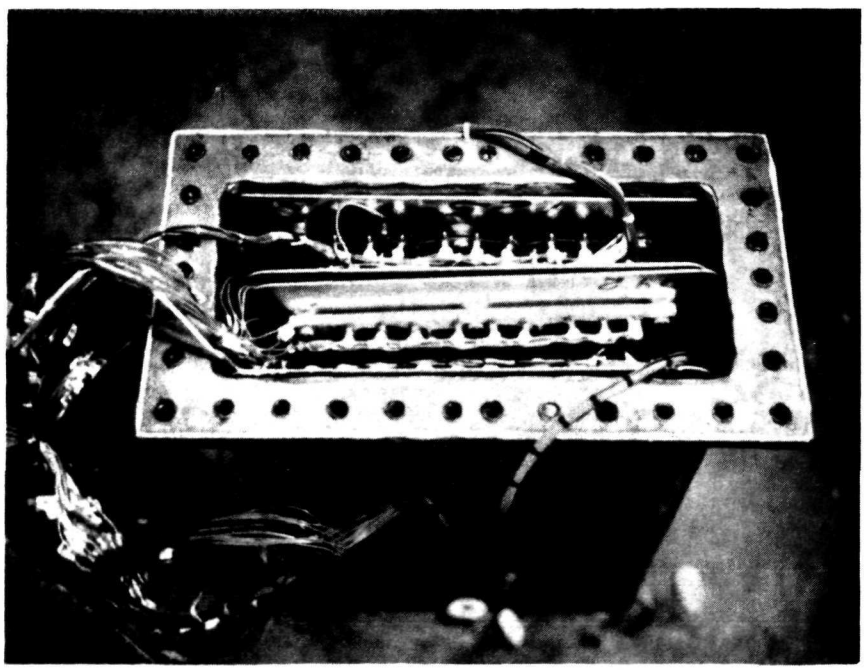

Fig. 29. Photograph of LN_2 Temperature Panels in Cold-Vacuum Chamber after Completion of Long-Term Test

top removed to expose the pressure panels. All of the cells in both facilities were pillowed, i.e., pressurized, and in their original, excellent condition. Some of these panels were returned to LRC for further examinations.

Discussion of an Anomaly - Soon after beginning the long-term experiment, Pressure Cell 11, Panel 114 (Weekly group, LN_2 temperature) registered a significant decrease in firing voltage. Within a month, the recorded weekly voltages decreased from approximately 1500 volts to approximately 1000 volts. Eventually, it fired during routine monitoring and continued to fire occasionally. It was removed from the long-term experiment, i.e., voltage excitation was removed; however, it was caused to fire occasionally during routine weekly firings by increasing the applied voltage until a firing event occurred. Firing voltages observed during these events were satisfactory.

When the long-term experiments were terminated, Cell 11 of Panel 114 was examined carefully for any anomaly. The cell was fully pressurized (no gas leakage had occurred), and its firing voltage was satisfactory. Panel 114 was unique in one respect. The external connections to the electrodes in the other seven test panels were coated with RTV during fabrication at LRC. The RTV was carefully primed and applied in such a way as to avoid any voids in the insulating RTV in accordance with LRC procedures. Panel 114, by contrast, was received without the RTV coating. Consequently, RTV was applied to the external portion of the electrodes of Panel 114 at RTI, and it was applied without priming.

When Cell 11 of Panel 114 was examined, it was observed that the spacing between the external, negative electrode and the transducer housing (positive, ground potential) was significantly less than in other electrodes examined, i.e., the spacing was approximately 20 mils whereas others examined were approximately 35 mils. This close spacing, coupled with the pointed geometry of the electrode, was favorable to arcing. Furthermore, the RTV coating was defective and a huge void existed between the negative electrode of Cell 11 and ground. Figure 30 is a photograph showing the electrode geometry after the RTV was removed.

For spacecraft applications, insulation must have an adequate breakdown rating (two to five times greater than required for ground applications). Additionally, the insulation must fit snugly onto the conductors and be free of voids, both within the insulation and between the insulation and the conductor. This is necessary to prevent the trapping of gas between the insulation and the conductor. Gas pockets in insulation or in potting compounds of conformal coatings are particularly hazardous because the boundary between the solid dielectric and a gas of lower dielectric constant gives rise to an increase in electrical stress on the gas. This is often enough to cause a breakdown in the gas, which in turn results in heating and decomposition of the adjacent insulation.

Fig. 30. Photograph of Internal Electrodes, Panel 114, Cell 11 after Removal of RTV.

Along with pressurization in sealed containers and conformal coatings, potting is frequently used in spacecraft to prevent voltage breakdown from occurring. The potting method is commonly used in long-term space flights, and potting with RTV was used on the long-term test panels. Potting procedures should insure that the parts of the system are scrupulously clean, and care must be exercised to avoid entrapment of gas in the potting compound or between the potting compound and the high voltage systems. A gas-filled void existing in an insulating material of higher dielectric constant will have an electric field many times greater than would occur in the gas alone or in a perfect solid insulator. When there are voids, the evolution of gas from the surrounding material may make the volume near high voltage components sufficiently conductive such that breakdown will readily occur. It is significant that some space centers avoid the use of RTV as much as possible because of outgassing problems and the difficulty of eliminating voids. When RTV is used, the normal procedure is to thin it with a priming material so as to reduce viscosity and evacuate to remove entrapped air. These precautions were not taken with the RTV application to Panel 114 at RTI and a void is known to have existed between the high voltage cathode and the transducer housing or ground [Ref. 4].

Conclusion - With respect to the firing of Cell 11, Panel 114, it is concluded that the breakdown occurred external to the cell. The reduced spacing between the external cathode and housing, the pointed geometry evident in Fig. 30, and the large void between the cathodes and housing were all conducive to an occasional, external firing event.

Although it is not considered an anomaly, one other observation is noted relative to the long-term experiment results. The firing voltages of Cell 3, Panel 114 were also observed to decrease significantly during the long-term experiment. After firing on a weekly schedule at voltages in the 1800-1900 volts range, the firing voltages were observed to decease to the 1000-1100 volts range. Concurrent with this decrease, pressure in the cold-vacuum chamber increased significantly as recorded on a thermocouple gauge. After the supporting vacuum system was serviced, the cold-vacuum chamber pressure returned to its normal, low value and the firing voltages of Cell 3 also returned to normal. Thus, the firing voltage recorded for Cell 3 was observed to be reversible with the decrease in pressure. Subsequently, it was demonstrated to be reversible with pressure. It is concluded that the low voltage firings recorded during periods of higher pressure were actually firings external to the pressure cell.

Slow Leak-Rate Response - Early Pioneer 10 results have generated an interest in the response of a pressure cell to an extremely slow leak. Significantly long time intervals, e.g., several minutes to more than one hour, have been observed between a first and second firing event when the leak was stopped following the initial firing event. However, the transducer broke into oscillation immediately or very shortly after the second event. An experiment with a controlled, slow leak has been set up that will give a profile of the transducer's response to the extremely slow leak. It will take some time to complete this experiment which is continuing.

"Page missing from available version"

SECTION V

SUMMARY AND CONCLUSIONS

As this report is being written, Pioneer 10 is nearing the end of the Asteroid Belt on its journey to the vicinity of Jupiter. Pioneer G is scheduled to be launched in March 1973 to follow a similar path. Both Pioneer 10 and Pioneer G are carrying the pressure cells described in this report as the sensors of a Meteoroid Detection Experiment (MDE). Considerable data has already been received from Pioneer 10 that may alter existing concepts of the nature of the Asteroid Belt. Subsequent reports from NASA will analyze the MDE data from both Pioneer 10 and Pioneer G and draw appropriate conclusions.

The MDE experiments of Pioneer 10 and Pioneer G are described in detail in this report and a preceding report [Ref. 1]. The investigations described in this report were primarily concerned with certain characteristics of the MDE sensors. In particular, the Paschen characteristics of the MDE pressure cells were investigated to further demonstrate their suitability for the MDE experiment. The use of Ni^{63} as an initial ionization source was further investigated to assure that while filling an essential need, it did not compromise the experiment in any way and that the actual quantity used was not critical. Experiments were conducted to demonstrate that the appreciable amount of firings conducted on a panel prior to its acceptance for flight did not significantly alter its characteristics. It was demonstrated that significant electrode geometry variations were tolerable and that the proton and heavy ions likely to be encountered in space would not compromise the pressure cell characteristics.

Prior to the fabrication of flight quality panels, a number of development panels were extensively tested to prove the validity of the fabrication procedure. Results from these tests suggested minor alterations in the fabrication procedure that enhanced the quality of the flight panels. Finally, flight quality panels were placed in a cold-vacuum environment and others were placed in a room-temperature vacuum environment. These were energized with 600 volts and continuously monitored for a period of one year. These test cells were periodically caused to fire by increasing the voltage applied to a test cell according to the schedule of Table IX.

The experimental results described in this report have demonstrated the suitability of the Pioneer 10/G MDE pressure panels or sensors. They have been demonstrated to be reliable and suitable for the long-term applications in the space environment required for the Pioneer 10/G missions.

"Page missing from available version"

REFERENCES

1. C. D. Parker, Evaluation of a Gas Discharge Transducer and Associated Instrumentation Necessary for the Asteroid Belt Meteoroid Experiment, NASA CR-111848, Research Triangle Institute, Research Triangle Park, North Carolina 27709, February 1971.

2. Pioneer F/G Project Specifications (PC-200, PC-213-00-03, PR-200, PS-201, PS-220), NASA, Ames Research Center, Moffett Field, California, April 10, 1969.

3. Private Communication, LRC personnel.

4. Vacuum Techniques, Saul Dushman, John Wiley and Sons, New York, 1949.

5. Paul, Fred W., et al., The Prevention of Electrical Breakdown in Spacecraft, NASA-SP-208, 1969.

"Page missing from available version"

APPENDIX A

TABULATION OF FIRING VOLTAGES OF LONG-TERM EXPERIMENT PRESSURE CELLS

"Page missing from available version"

APPENDIX A

TABULATION OF FIRING VOLTAGES OF LONG-TERM EXPERIMENT PRESSURE CELLS

Firing voltages of the long-term experiment pressure cells are tabulated in this appendix. Table A-1 is a tabulation of results from the weekly group in the cold-vacuum facility. The single anomaly to occur during this experiment occurred in this group, i.e., Cell 11, Panel 114. This cell was removed from the experiment after the 1/20/72 firing; however, it was occasionally fired after that date, and these results are recorded in the table. Other results are tabulated as follows:

Table A-2; Weekly group, room temperature
Table A-3; Monthly group, LN_2 temperature
Table A-4; Monthly group, room temperature
Table A-5; 12-week group, LN_2 temperature
Table A-6; 12-week group, room temperature
Table A-7; 24-week group, LN_2 temperature
Table A-8; 24-week group, room temperature
Table A-9; 48 week group, LN_2 temperature
Table A-10; 48-week group, room temperature
Table A-11; Unscheduled group, LN_2 temperature
Table A-12; Unscheduled group, room temperature.

The tabulations in this appendix do not include firing results prior to the long-term test or terminating results after the long-term tests were concluded. These data are summarized in Section IV, Tables X through XVII of this report. In some instances, i.e., Tables A-9 through A-12, this means that only the several firings recorded at the conclusion of the long-term tests are tabulated.

TABLE A-1

Firing Voltages of Pressure Cells on a Weekly Test Schedule

(T = Liquid Nitrogen)

Panel,	Cell No.	11/5	11/12	11/18	11/21	12/2
092	1	1340	1340	1440	1300	1370
	2	1380	1490	1460	1420	1490
	10	1380	1360	1470	1420	1460
114	3	1780	1680	1860	1810	1660
	11	1550	1450	1200	1020	900
	12	1670	1780	1810	1770	1610
125	4	1270	1430	1430	1350	1350
	5	1390	1470	1470	1430	1490
	13	1360	1490	1490	1400	1450
154	6	1360	1430	1480	1430	1510
	14	1380	1550	1540	1460	1520
	15	1370	1490	1500	1470	1480

TABLE A-1
(Continued)
Firing Voltages of Pressure Cells on a
Weekly Test Schedule

(T = Liquid Nitrogen)

Panel,	Cell No.	12/9	12/16	12/23	12/30	1/6/72
092	1	1430	1430	1360	1410	1440
	2	1500	1490	1500	1580	1580
	10	1470	1440	1420	1470	1490
114	3	1580	1350	1560	1400	1300
	11	1130	1080	1180	900	1000
	12	1790	1780	1800	1840	1800
125	4	1340	1360	1300	1280	1360
	5	1470	1470	1480	1450	1470
	13	1500	1490	1450	1450	1460
154	6	1530	1510	1490	1470	1500
	14	1500	1540	1480	1520	1540
	15	1540	1520	1480	1500	1530

TABLE A-1
(Continued)
Firing Voltage of Pressure Cells on a
Weekly Test Schedule

(T = Liquid Nitrogen)

Panel,	Cell No.	1/13	1/20	1/27	2/3	2/10
092	1	1470	1390	1420	1360	1420
	2	1500	1550	1550	1500	1520
	10	1480	1470	1540	1490	1530
114	3	1280	1350	1460	1800	1430
	11	1110	950			
	12	1780	1810	1780	1860	1790
125	4	1340	1320	1390	1350	1400
	5	1490	1460	1450	1470	1490
	13	1460	1450	1480	1460	1470
154	6	1460	1490	1500	1480	1530
	14	1520	1530	1520	1520	1530
	15	1550	1540	1500	1480	1490

TABLE A-1
(Continued)
Firing Voltages of Pressure Cells on a
Weekly Test Schedule

(T = Liquid Nitrogen)

Panel,	Cell No.	2/17	2/24	3/2	3/9	3/16
092	1	1370	1430	1330	1370	1380
	2	1460	1510	1490	1490	1560
	10	1460	1480	1390	1430	1450
114	3	1800	1850	1600	1660	1780
	11	900				
	12	1800	1700	1600	1710	1710
125	4	1390	1310	1280	1320	1280
	5	1480	1400	1310	1390	1410
	13	1480	1400	1320	1400	1420
154	6	1510	1440	1390	1430	1440
	14	1540	1410	1350	1440	1450
	15	1500	1450	1390	1420	1500

TABLE A-1
(Continued)
Firing Voltages of Pressure Cells on a
Weekly Test Schedule

(T = Liquid Nitrogen)

Panel,	Cell No.	3/23	3/30	4/6/72	4/13	4/20
092	1	1360	1360	1380	1410	1390
	2	1500	1510	1490	1510	1500
	10	1490	1460	1490	1480	1450
114	3	1890	1810	1910	1890	1910
	11			1200	1720	1680
	12	1820	1760	1810	1740	1700
125	4	1310	1270	1410	1390	1400
	5	1430	1460	1470	1450	1430
	13	1420	1450	1460	1470	1450
154	6	1510	1470	1470	1520	1520
	14	1510	1550	1530	1560	1540
	15	1500	1530	1510	1510	1540

TABLE A-1
(Continued)
Firing Voltages of Pressure Cells on a
Weekly Test Schedule

(T = Liquid Nitrogen)

Panel,	Cell No.	4/27	5/4	5/11	5/18	5/25
092	1	1400	1380	1350	1360	1430
	2	1570	1570	1570	1460	1520
	10	1450	1430	1480	1430	1510
114	3	1980	1870	1870	1800	1940
	11	1360	1760	1200	1700	1730
	12	1640	1830	1830	1760	1640
125	4	1370	1430	1420	1330	1380
	5	1460	1460	1490	1390	1471
	13	1440	1500	1450	1370	1420
154	6	1500	1480	1490	1440	1480
	14	1540	1530	1560	1410	1500
	15	1530	1500	1520	1430	1500

TABLE A-1
(Continued)
Firing Voltages of Pressure Cells on a
Weekly Test Schedule

(T = Liquid Nitrogen)

Panel,	Cell No.	6/1	6/8	6/15	6/22	6/29
092	1	1350	1360	1420	1360	1400
	2	1560	1530	1540	1590	1600
	10	1510	1550	1510	1500	1530
114	3	1850	1910	1870	1940	1960
	11	1730	1300	1740	--	--
	12	1740	1620	1800	1800	1920
125	4	1310	1500	1400	1390	1380
	5	1460	1510	1520	1510	1490
	13	1420	1440	1460	1440	1480
154	6	1470	1530	1490	1500	1500
	14	1520	1520	1520	1530	1540
	15	1530	1550	1500	1520	1530

TABLE A-1
(Continued)
Firing Voltages of Pressure Cells on a
Weekly Test Schedule

(T = Liquid Nitrogen)

Panel,	Cell No.	7/6	7/20	7/27	8/2	8/10
92	1	1400	1410	1450	1380	1480
	2	1570	1540	1510	1570	1500
	10	1500	1550	1540	1510	1550
114	3	1880	1900	1990	1980	1190
	11	--	--	--	--	--
	12	1870	1840	1820	1820	1760
125	4	1440	1410	1480	1410	1460
	5	1510	1490	1500	1480	1280
	13	1470	1470	1470	1490	1460
154	6	1510	1470	1510	1510	1500
	14	1530	1530	1520	1530	1550
	15	1500	1520	1470	1490	1500

TABLE A-1
(Continued)
Firing Voltages of Pressure Cells on a
Weekly Test Schedule

(T = Liquid Nitrogen)

Panel,	Cell No.	8/18	8/24	8/31	9/7	9/14
92	1	1380	1330	1410	1390	1430
	2	1570	1570	1570	1580	1570
	10	1520	1500	1510	1530	1430
114	3	1300	1520	1160	1010	1880
	11	--	--	--	--	--
	12	1830	1780	1760	1700	1800
125	4	1430	1460	1410	1450	1450
	5	1350	1330	1070	950	1470
	13	1480	1490	1450	1460	1490
154	6	1540	1510	1510	1520	1520
	14	1550	1520	1520	1570	1540
	15	1520	1520	1530	1530	1510

TABLE A-1
(Continued)
Firing Voltages of Pressure Cells on a
Weekly Test Schedule

(T = Liquid Nitrogen)

Panel,	Cell No.	9/18	9/19	9/20
92	1	1450	1390	1420
	2	1560	1590	1520
	10	1500	1490	1500
114	3	1930	1900	1810
	11	--	--	--
	12	1790	1850	1800
125	4	1430	1420	1440
	5	1480	1530	1490
	13	1460	1500	1460
154	6	1550	1510	1490
	14	1540	1520	1520
	15	1530	1510	1520

TABLE A-2

Firing Voltages of Pressure Cells on a Weekly Test Schedule

(T = 25°C)

Panel,	Cell No.	11/5	11/12	11/18	11/21	12/2
137	2	1330	1330	1310	1320	1350
	3	1290	1280	1290	1280	1290
	10	1270	1220	1320	1270	1240
146	5	1210	1200	1250	1200	1200
	11	1230	1260	1240	1290	1270
	12	1230	1230	1230	1230	1240
151	5	1200	1200	1190	1180	1160
	8	1220	1220	1200	1230	1230
	13	1080	1070	1070	1080	1090
161	9	1220	1370	1350	1330	1340
	14	1350	1350	1350	1340	1360
	15	1360	1390	1360	1350	1370

TABLE A-2
(Continued)
Firing Voltages of Pressure Cells on a
Weekly Test Schedule

(T = 25°C)

Panel,	Cell No.	12/9	12/16	12/23	12/30	1/6/72
137	2	1340	1340	1320	1300	1290
	3	1300	1270	1290	1280	1300
	10	1280	1280	1250	1280	1290
146	5	1230	1220	1220	1250	1240
	11	1250	1250	1240	1290	1260
	12	1250	1240	1260	1230	1240
151	5	1180	1190	1160	1200	1150
	8	1220	1240	1200	1230	1210
	13	1060	1070	1130	1080	1100
161	9	1350	1370	1360	1340	1360
	14	1370	1360	1350	1330	1340
	15	1380	1380	1370	1350	1380

TABLE A-2
(Continued)
Firing Voltages of Pressure Cells on a
Weekly Test Schedule

(T = 25°C)

Panel,	Cell No.	1/13	1/20	1/27	2/3	2/10	2/17
137	2	1310	1330	1340	1330	1320	1330
	3	1290	1300	1260	1280	1300	1290
	10	1270	1260	1270	1280	1290	1260
146	5	1210	1200	1190	1210	1200	1190
	11	1240	1220	1210	1230	1210	1220
	12	1260	1240	1240	1250	1240	1250
151	5	1150	1150	1190	1180	1170	1180
	8	1190	1200	1200	1210	1200	1200
	13	1110	1160	1110	1120	1160	1150
161	9	1340	1350	1340	1360	1320	1330
	14	1340	1350	1350	1340	1350	1340
	15	1370	1340	1360	1380	1370	1360

TABLE A-2
(Continued)
Firing Voltages of Pressure Cells on a
Weekly Test Schedule

(T = 25°C)

Panel,	Cell No.	2/24	3/2	3/9	3/16	3/23
137	2	1310	1320	1330	1320	1320
	3	1300	1290	1280	1250	1270
	10	1270	1280	1260	1300	1290
146	5	1200	1200	1200	1210	1210
	11	1210	1220	1230	1180	1200
	12	1240	1230	1250	1230	1240
151	5	1170	1180	1190	1170	1180
	8	1190	1190	1190	1210	1200
	13	1130	1160	1140	1180	1170
161	9	1350	1320	1360	1320	1340
	14	1350	1360	1340	1340	1330
	15	1380	1370	1370	1370	1360

TABLE A-2
(Continued)
Firing Voltages of Pressure Cells on a
Weekly Test Schedule

(T = 25°C)

Panel,	Cell No.	3/30	4/6	4/13	4/20	4/27
137	2	1330	1320	1290	1310	1300
	3	1260	1260	1300	1280	1260
	10	1290	1300	1240	1280	1250
146	5	1200	1210	1230	1220	1220
	11	1190	1200	1200	1200	1220
	12	1220	1250	1240	1210	1250
151	5	1180	1190	1210	1200	1160
	8	1190	1210	1190	1200	1220
	13	1160	1180	1190	1180	1210
161	9	1310	1350	1320	1340	1330
	14	1320	1320	1300	1320	1320
	15	1360	1360	1350	1360	1380

TABLE A-2
(Continued)
Firing Voltages of Pressure Cells on a
Weekly Test Schedule
(T = 25°C)

Panel,	Cell No.	5/4	5/11	5/18	5/25	6/1
137	2	1310	1300	1300	1300	1300
	3	1290	1300	1250	1270	1290
	10	1270	1240	1290	1280	1250
146	5	1210	1230	1220	1190	1230
	11	1200	1210	1210	1220	1230
	12	1230	1250	1220	1220	1250
151	5	1180	1200	1170	1190	1160
	8	1200	1190	1200	1200	1210
	13	1190	1200	1160	1160	1190
161	9	1340	1330	1370	1360	1360
	14	1300	1300	1360	1340	1320
	15	1370	1380	1380	1380	1360

TABLE A-2
(Continued)
Firing Voltages of Pressure Cells on a
Weekly Test Schedule
(T = 25°C)

Panel,	Cell No.	6/8	6/15	6/22	6/29	7/6
137	2	1330	1340	1320	1300	1300
	3	1270	1270	1280	1270	1290
	10	1230	1290	1270	1290	1250
146	5	1200	1200	1200	1210	1200
	11	1200	1200	1180	1220	1230
	12	1230	1230	1230	1220	1220
151	5	1130	1150	1170	1180	1110
	8	1210	1200	1190	1190	1190
	13	1160	1160	1140	1120	1140
161	9	1360	1350	1350	1350	1340
	14	1310	1310	1360	1300	1350
	15	1360	1350	1335	1330	1350

TABLE A-2
(Continued)
Firing Voltages of Pressure Cells on a
Weekly Test Schedule
(T = 25°C)

Panel,	Cell No.	7/20	7/27	8/2	8/10	8/18
137	2	1300	1330	1310	1320	1300
	3	1280	1250	1270	1270	1270
	10	1310	1290	1270	1230	1310
146	5	1190	1200	1200	1220	1210
	11	1190	1210	1190	1160	1160
	12	1230	1240	1270	1220	1230
151	5	1180	1130	1150	1190	1190
	8	1220	1180	1200	1190	1210
	13	1140	1120	1120	1130	1120
161	9	1350	1380	1350	1320	1350
	14	1310	1300	1340	1330	1310
	15	1370	1340	1320	1360	1350

TABLE A-2
(Continued)
Firing Voltages of Pressure Cells on a
Weekly Test Schedule
(T = 25°C)

Panel,	Cell No.	8/24	8/31	9/7	9/14	9/18
137	2	1310	1340	1330	1330	1320
	3	1290	1270	1290	1250	1250
	10	1250	1230	1270	1280	1240
146	5	1200	1190	1210	1210	1210
	11	1160	1210	1190	1190	1200
	12	1230	1230	1260	1220	1250
151	5	1180	1160	1140	1180	1150
	8	1200	1190	1250	1200	1180
	13	1130	1160	1130	1140	1120
161	9	1360	1340	1370	1340	1330
	14	1310	1330	1310	1320	1320
	15	1340	1360	1360	1340	1370

TABLE A-2
(Continued)
Firing Voltages of Pressure Cells on a
Weekly Test Schedule

(T = 25°C)

Panel,	Cell No.	9/19	9/20	
137	2	1340	1310	
	3	1270	1300	
	10	1220	1240	
146	5	1200	1210	
	11	1190	1220	
	12	1260	1250	
151	5	1170	1130	
	8	1190	1190	
	13	1120	1130	
161	9	1370	1380	
	14	1310	1290	
	15	1350	1340	

TABLE A-3

Firing Voltages of Pressure Cells on a Monthly Test Schedule

(T = Liquid Nitrogen)

Panel,	Cell No.	11/12	12/9	1/6/72	1/27	2/24
092	3	1440	1430	1440	1450	1400
	11	1400	1430	1450	1490	1450
	12	1450	1450	1480	1500	1440
114	4	1690	1700	1720	1770	1650
	5	1760	1770	1760	1750	1670
	13	1750	1740	1760	1790	1690
125	6	1380	1440	1460	1510	1370
	14	1310	1350	1380	1410	1360
	15	1260	1340	1400	1420	1320
154	7	1490	1500	1490	1570	1460
	8	1550	1600	1620	1620	1560
	16	1390	1440	1440	1530	1460

TABLE A-3
(continued)
Firing Voltages of Pressure Cells on a
Monthly Test Schedule

(T = Liquid Nitrogen)

Panel,	Cell No.	3/30	5/4	6/1	6/30	7/27	8/25
092	3	1340	1460	1400	1460	1480	1490
	11	1410	1520	1400	1490	1480	1510
	12	1450	1550	1450	1550	1540	1530
114	4	1640	1740	1660	1750	1810	1740
	5	1640	1690	1640	1800	1840	1740
	13	1710	1790	1720	1790	1780	1800
125	6	1340	1420	1340	1480	1520	1500
	14	1300	1380	1420	1410	1380	1390
	15	1280	1400	1310	1460	1450	1510
154	7	1450	1490	1430	1540	1530	1490
	8	1550	1610	1600	1620	1670	1620
	16	1440	1510	1460	1560	1520	1550

TABLE A-3
(Continued)
Firing Voltages of Pressure Cells on a
Monthly Test Schedule

(T = Liquid Nitrogen)

Panel, Cell No.		9/18	9/19	9/20	
092	3	1530	1480	1440	
	11	1530	1480	1480	
	12	1510	1530	1530	
114	4	1750	1760	1810	
	5	1800	1760	1810	
	13	1780	1800	1820	
125	6	1540	1530	1550	
	14	1380	1420	1400	
	15	1490	1470	1500	
154	7	1560	1510	1560	
	8	1650	1640	1620	
	16	1550	1520	1520	

TABLE A-4

Firing Voltages of Pressure Cells on a Monthly Test Schedule

(T = 25°C)

Panel,	Cell No.	11/12	12/9	1/6/72	1/27	2/24
137	4	1270	1250	1240	1270	1250
	11	1320	1330	1320	1310	1330
	12	1270	1250	1300	1290	1280
146	6	1230	1230	1260	1260	1250
	7	1190	1170	1210	1200	1210
	13	1140	1150	1150	1150	1140
151	9	1160	1130	1240	1150	1160
	14	1150	1150	1150	1180	1150
	15	1180	1180	1140	1200	1190
161	10	1410	1430	1420	1400	1410
	11	1370	1370	1350	1380	1360
	16	1310	1330	1280	1260	1290

TABLE A-4
(continued)
Firing Voltages of Pressure Cells on a
Monthly Test Schedule

(T = 25°C)

Panel,	Cell No.	3/30	5/4	6/1	6/30	7/27	8/25
137	4	1240	1280	1230	1230	1240	1220
	11	1320	1320	1360	1310	1300	1300
	12	1250	1300	1240	1260	1280	1260
146	6	1230	1260	1240	1230	1240	1210
	7	1170	1210	1160	1210	1200	1200
	13	1150	1160	1140	1160	1140	1140
151	9	1140	1200	1160	1130	1130	1170
	14	1170	1180	1160	1150	1170	1160
	15	1160	1170	1160	1150	1160	1150
161	10	1390	1420	1400	1420	1400	1410
	11	1380	1370	1360	1360	1380	1370
	16	1340	1330	1330	1320	1300	1290

TABLE A-4
(continued)
Firing Voltages of Pressure Cells on a
Monthly Test Schedule

(T = 25°C)

Panel,	Cell No.	9/18	9/19	9/20
137	4	1240	1230	1260
	11	1310	1330	1320
	12	1300	1270	1260
146	6	1210	1220	1230
	7	1170	1160	1200
	13	1140	1110	1110
151	9	1180	1170	1150
	14	1140	1160	1150
	15	1180	1150	1180
161	10	1410	1400	1400
	11	1370	1360	1370
	16	1280	1320	1310

TABLE A-5

Firing Voltages of Pressure Cells on a
12 Week Test Schedule

(T = Liquid Nitrogen)

Panel,	Cell No.	1/27/72	4/13	7/6	9/18	9/19	9/20
092	4	1370	1400	1400	1450	1490	1470
	6	1340	1360	1370	1410	1460	1410
	13	1410	1370	1390	1490	1480	1500
114	6	1630	1560	1610	1730	1730	1730
	14	1530	1570	1630	1750	1690	1660
	15	1480	1700	1750	1830	1850	1840
125	7	1370	1410	1350	1430	1460	1480
	8	1370	1410	1380	1450	1480	1530
	16	1410	1320	1360	1450	1470	1510
154	9	1520	1460	1450	1550	1510	1660
	17	1460	1440	1480	1560	1560	1550
	18	1380	1330	1360	1450	1430	1470

TABLE A-6

Firing Voltages of Pressure Cells on a
12 Week Test Schedule

(T = 25°C)

Panel,	Cell No.	1/27/72	4/13	7/6	9/18	9/19	9/20
137	5	1150	1170	1140	1150	1170	1150
	6	1300	1190	1250	1280	1290	1280
	13	1270	1240	1270	1290	1300	1270
146	8	1190	1210	1190	1210	1180	1130
	14	1210	1190	1190	1180	1160	1180
	15	1240	1230	1200	1180	1210	1180
151	1	1170	1210	1160	1180	1160	1190
	2	1280	1240	1250	1220	1250	1230
	16	1250	1280	1270	1240	1250	1200
161	1	1250	1310	1220	1230	1210	1200
	17	1350	1200	1260	1250	1280	1280
	18	1290	1270	1350	1320	1360	1340

TABLE A-7

Firing Voltages of Pressure Cells on a
24 Week Test Schedule

(T = Liquid Nitrogen)

Panel,	Cell No.	5/4/72	9/18	9/19	9/20
092	7	1410	1430	1540	1490
	14	1330	1380	1450	1430
	15	1440	1430	1520	1510
114	7	1660	1660	1810	1780
	8	1620	1670	1850	1750
	16	1560	1630	1650	1650
125	9	1350	1330	1390	1410
	18	1280	1320	1410	1420
	10	1300	1360	1470	1440
154	1	1370	1400	1480	1510
	2	1410	1480	1570	1550
	10	1370	1410	1540	1460

TABLE A-8

Firing Voltages of Pressure Cells on a
24 Week Test Schedule

(T = 25°C)

Panel,	Cell No.	5/4/72	9/18	9/19	9/20
137	7	1230	1300	1300	1270
	14	1260	1240	1230	1300
	15	1270	1270	1240	1280
146	1	1450	1440	1460	1440
	2	1300	1240	1230	1240
	16	1210	1210	1220	1180
151	3	1210	1190	1210	1210
	17	1210	1180	1190	1170
	18	1140	1130	1120	1110
161	2	1330	1330	1360	1300
	3	1290	1270	1270	1280
	12	1320	1280	1270	1320

TABLE A-9

Firing Voltages of Pressure Cells on a 48-Week Test Schedule

(T = Liquid Nitrogen)

Panel,	Cell No.	9/18/72	9/19	9/20
092	8	1420	1520	1550
	9	1410	1530	1550
	16	1380	1450	1520
114	9	1840	1920	1960
	17	1640	1660	1600
	18	1430	1400	1170
125	1	1400	1430	1320
	2	1260	1440	1430
	11	1320	1480	1500
154	3	1430	1560	1570
	11	1410	1530	1560
	12	1300	1450	1500

TABLE A-10

Firing Voltages of Pressure Cells on a
48-Week Test Schedule

(T = 25° C)

Panel,	Cell No.	9/18/72	9/19	9/20
137	8	1250	1240	1230
	9	1310	1290	1300
	16	1190	1200	1200
146	3	1260	1240	1280
	17	1130	1140	1140
	18	1090	1120	1140
151	4	1160	1140	1170
	10	1210	1200	1230
	11	1250	1220	1240
161	4	1280	1320	1310
	5	1250	1290	1240
	8	1280	1280	1290

TABLE A-11

Firing Voltages of Pressure Cells in the Unscheduled Group

(T = Liquid Nitrogen)

Panel,	Cell No.	9/18/72	9/19	9/20
092	17	1450	1520	1550
	18	1310	1400	1410
114	2	1650	1800	1880
	10	1580	1740	1760
125	3	1280	1440	1360
	12	1290	1450	1470
154	4	1380	1520	1410
	5	1420	1540	1520
	13	1320	1450	1550

TABLE A-12

Firing Voltages of Pressure Cells in the Unscheduled Group

(T = 25° C)

Panel,	Cell No.	9/18/72	9/19	9/20
137	17	1260	1280	1280
	18	1600	1560	1570
146	10	1230	1290	1260
151	12	1190	1210	1260
161	6	1280	1270	1300
	7	1340	1350	1360
	13	1330	1340	1360

"Page missing from available version"

APPENDIX B

SIMULATION OF HEAVY ION AND PROTON IRRADIATION EFFECTS ON THE MDE GAS DISCHARGE TRANSDUCER

"Page missing from available version"

EXPERIMENTAL PROGRAM TO DETERMINE LONG-TERM

CHARACTERISTICS OF THE MDE PRESSURE TRANSDUCERS

SIMULATION OF HEAVY ION AND PROTON IRRADIATION

EFFECTS ON THE MDE GAS DISCHARGE TRANSDUCER

By L. K. Monteith

April 1972

Contract No. NAS1-10175
RTI No. 43U-568

Prepared for

National Aeronautics and Space Administration
Langley Research Center
Hampton, Virginia 23365

"Page missing from available version"

SIMULATION OF HEAVY ION AND PROTON IRRADIATION EFFECTS ON THE MDE GAS DISCHARGE TRANSDUCER

INTRODUCTION

Two possible radiation effects which could result in spurious outputs from the MDE gas discharge transducer are suggested. The radiation induced ionization could be collected in the applied field and result in a voltage pulse across the transducer. Secondly, the induced ionization could reduce the field required to sustain avalanche multiplication. A detailed analysis of either effect is beyond the scope of this discussion, however, a simple analysis will be presented later as a means to interpret the data.

Without a detailed model for the interaction of irradiation with the gas discharge transducer and without reliable data on the heavy ion and proton energy and fluence expected in flight, a purely empirical test program was devised to simulate worst case conditions. Four gas discharge transducers were exposed to a pulsed beam of 576 MeV protons at average flux rates near 10^{10} protons/cm^2-sec. The instantaneous flux rate was nearly 200 times the average rate and the pulse width was approximately 100 microseconds occurring at 55 cycles per second. The proton flux covered a 1 in^2 area. The uniformity of the beam was assessed visually and the average flux rate was monitored by a Faraday cup.

The gas discharge transducers were connected electrically as illustrated in Fig. B-1.

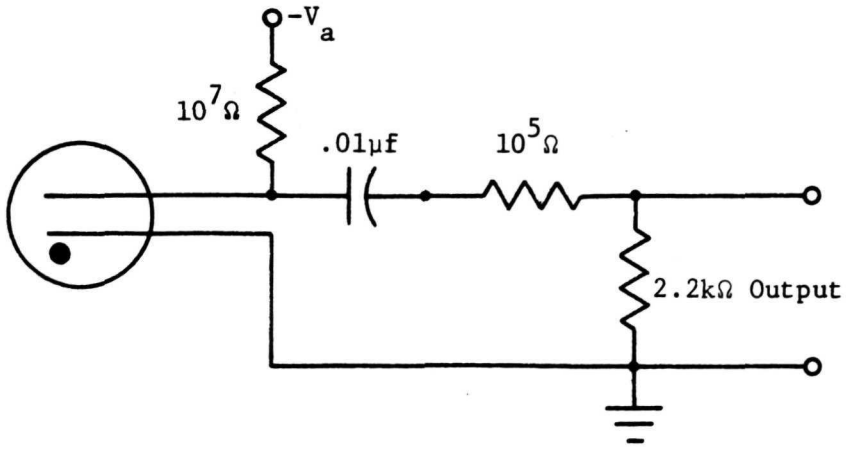

Fig. B-1. Schematic of Electrical Circuit for Gas Discharge Transducer During Irradiation Tests

Briefly, most of the measurements consisted of an electronic switch or gate which was actuated with a voltage pulse greater than two volts. The switch turned on a lamp as an indication of breakdown of the gas discharge transducer. The lamp glow was used as an indication that the transducer had discharged. In addition, the voltage across the 2.2 K resistor during the proton pulse was observed on occasion using an oscilloscope. The applied voltages across the transducer included both avalanche and non-avalanche conditions.

Experimental Results

Using the electronic switch as an indicator for transducer discharge, four transducers were exposed to 575 MeV protons with fluences covering the range from 10^9 to 10^{10} protons/cm^2-sec. The results are shown in Table B-I. From this data it is obvious that the proton flux had an effect upon the firing or discharge voltage of the transducer in the test configuration. Even though the magnitude of the voltage decrease is hundreds of volts, the percent charge is the order of 10 percent or less of the firing voltage without radiation. This is evident from Figure B-2 where the effect of the proton flux on the firing voltage is not very pronounced. Over the limited range of data a straight line relationship on the log-log plot appears to be an adequate fit. Then we have

$$V_f = \Phi^{-n}$$

where $n \simeq 0.07$ by fitting a straight line to the data. The major features of this result are that the firing voltage is reduced in a highly ionizing radiation environment; however, the effect of ionizing radiation on the firing voltage is not substantial over the range of the experiment. In fact, under the test conditions, the radiation would have no effect upon the performance of the discharge transducer as a pressure switch in the mode of operation intended for flight.

In an attempt to study charge collection of ionizing radiation the oscilloscope was used to observe the voltage developed across the 2.2 K resistor in Figure B-1. The observed voltage pulses were the order of tens of millivolts. Considering the voltage division across the 10^5 Ω resistor, the voltage developed across the transducer during the proton pulse was the order of volts at the maximum flux rate. Shown in Figure B-3 is the magnitude of the current pulse through the 2.2 K resistor as a function of applied field. It is obvious that the collected charge during the proton pulse will not be sufficient to develop the 2 volts necessary to switch the electronic circuit and yield a false firing.

TABLE B-I

Transducer Firing Voltages for Various Proton Flux Rates

Transducer Number	Flux Rate (Protons/cm^2 sec)	Firing Voltages (Volts)
37	0	1520-1540-1550-1560
	0.36×10^{10}	1490-1500-1510
	1.6×10^{10}	1450-1450-1450
	3.3×10^{10}	1280-1290-1310-1320
36	0	1350-1360-1370-1400
	3.4×10^{10}	1140-1200
19	0	1430
	3.3×10^{10}	1090-1100
4	0	1490
	0.19×10^{10}	1460-1460-1460
	0.42×10^{10}	1420-1420-1420
	0.68×10^{10}	1370-1370-1370
	1.7×10^{10}	1250-1250-1250
	3.4×10^{10}	1200-1210-1230

This was verified by actually observing the firing event as the applied voltage was increased across the transducer. However, the firing event was always coincident with the proton flux which further substantiated the influence of ionizing radiation upon the firing voltage.

As expected the collected charge is linearly related to the flux rate as shown in Figure B-4. Therefore, it may be assumed that during the 100 microsecond pulse of protons the ion-electron density reaches steady state. Therefore, the conductivity of the gas should be controlled by the flux rate, the lifetime of the ion electron pairs and the mobility of the ions and electrons. In addition, the instantaneous flux rate should be considered instead of the average flux rate in the interpretation of the results.

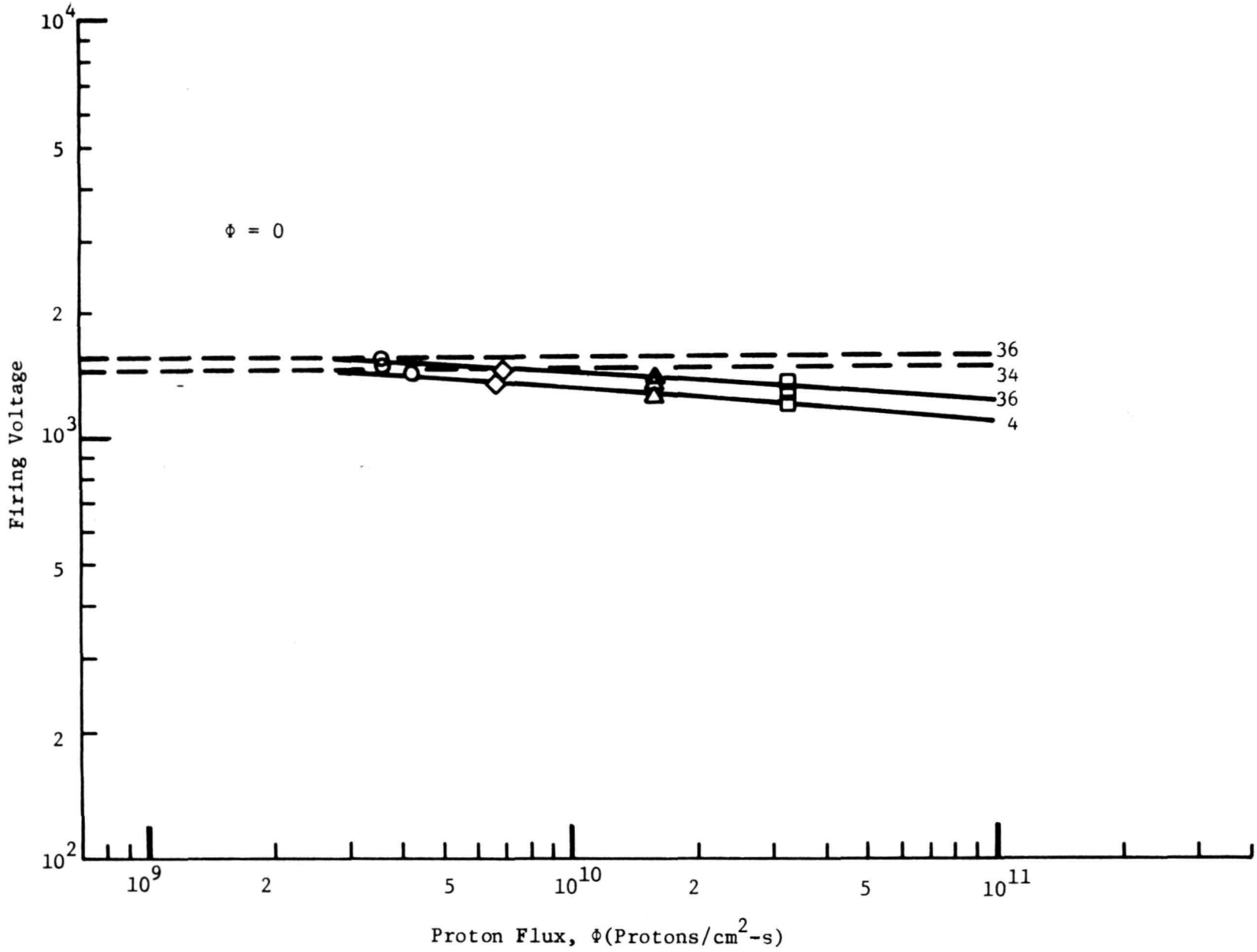

Fig. B-2. Firing Voltage Versus Proton Flux

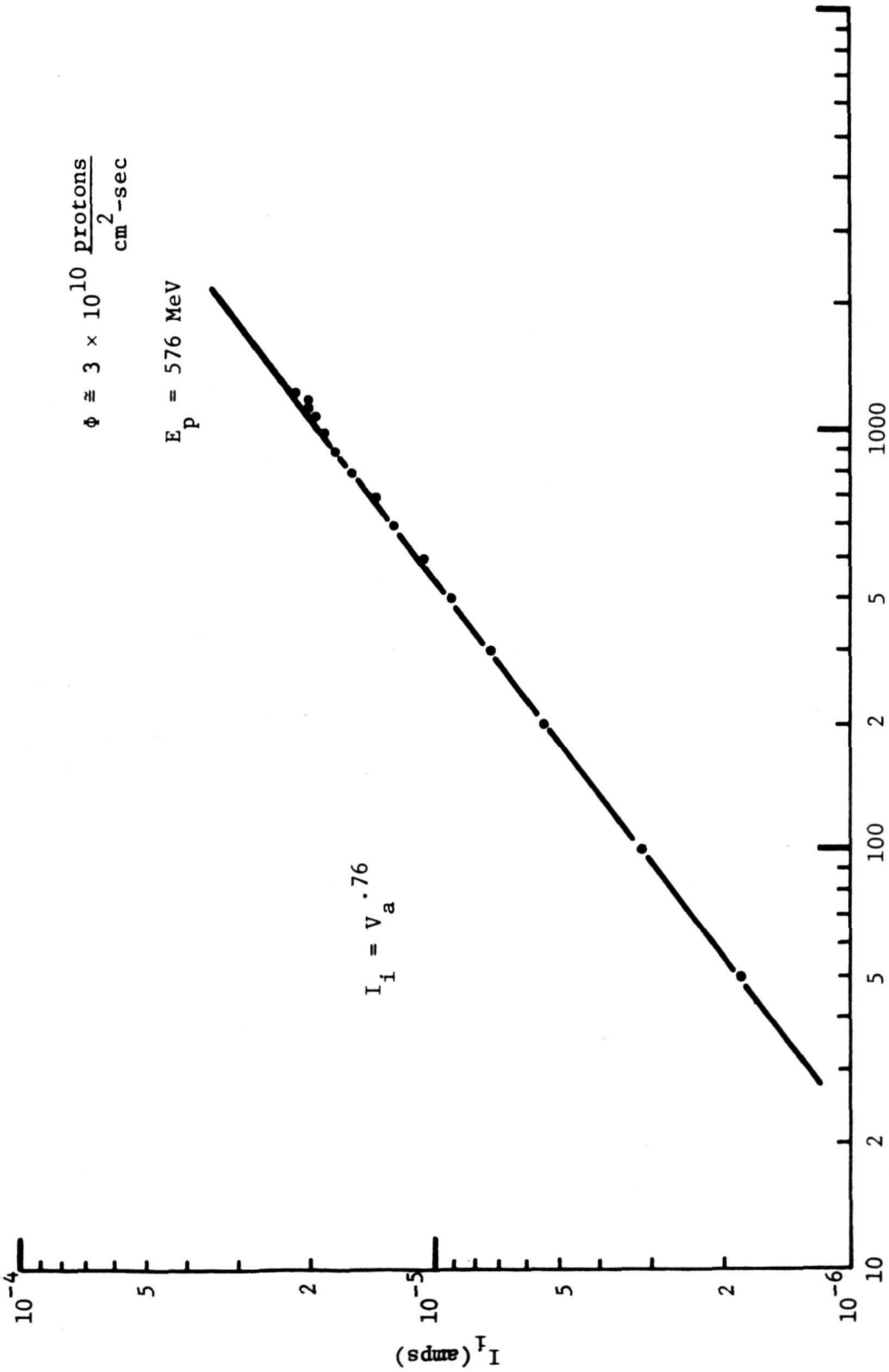

Fig. B-3. Magnitude of Current Pulse through the 2.2 kΩ Resistor Versus Applied Field

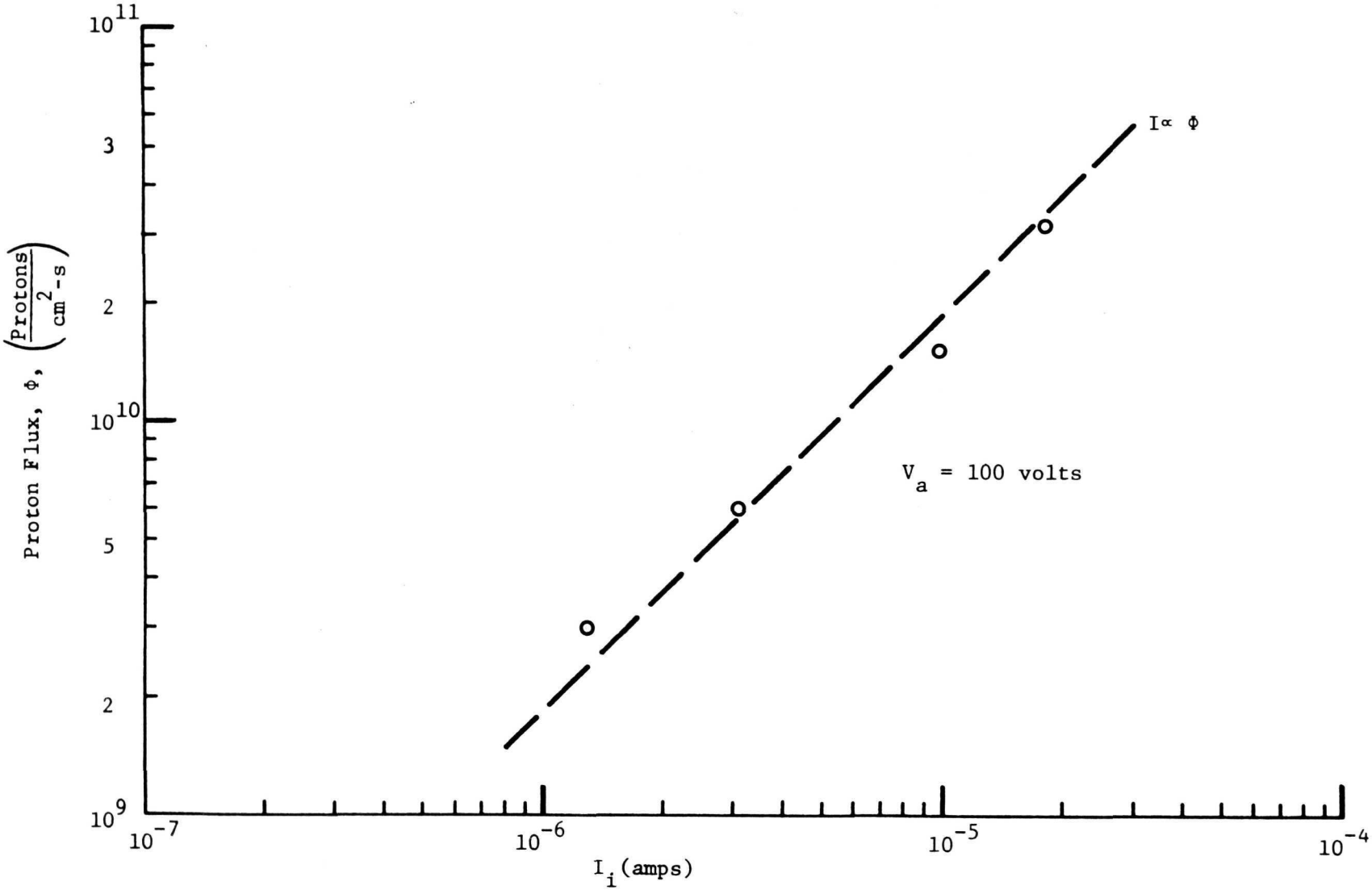

Fig. B-4. Proton Flux Rate Versus Collected Charge

Analysis

The primary consideration has to be the simulation. How does the energy and flux rate relate to the space environment? Again, a worst-case analysis is used. The major factor will be the energy loss by the protons in traversing the transducer. The mass stopping power versus energy for protons is available from numerous sources. The energy loss per unit path length is related to the mass stopping power by

$$\frac{1}{\rho}\ \frac{\partial E}{\partial x} = \frac{\partial E}{\partial \xi}\ ,$$

where

ρ is the density of the absorbing medium,

$\frac{\partial E}{\partial x}$ is the rate of energy loss per unit path length, and

$\frac{\partial E}{\partial \xi}$ is the mass stopping power.

For protons $\frac{\partial E}{\partial \xi}$ varies from approximately 0.2 MeV mg^{-1}-cm^2 at 1 MeV to 0.002 MeV mg^{-1}-cm^2 at 1 BeV. At 576 MeV, $\frac{\partial E}{\partial \xi}$ is also near 0.002 MeV mg^{-1}-cm^2. The rate of energy loss could be increased by going to lower energies, however, the flux rate for the SREL system decreased for lower energies faster than the increase in $\frac{\partial E}{\partial \xi}$. Therefore, using the high energy maximum ionization density in the gas was achieved.

Proton simulation is rather obvious. If the predominant energy of the protons encountered in space is near 1 MeV, the simulation should be scaled by the ratio of $\frac{\partial E}{\partial \xi}$ at 1 MeV to $\frac{\partial E}{\partial \xi}$ at 576 MeV and the flux rate for worst case simulation reduced by this factor. Specifically, at 30 MeV, $\frac{\partial E}{\partial \xi}$ = 0.015 MeV mg^{-1}-cm^2 and at 576 MeV, $\frac{\partial E}{\partial \xi}$ = 0.002 MeV mg^{-1}-cm^2. Using an average flux rate of 3×10^{10} protons/cm^2-sec corresponds to an instantaneous flux rate near 10^{12} protons/cm^2-sec. Therefore, the 576 MeV irradiations approximate the ionization effects of 30 MeV protons with a flux rate near 10^{11} protons/cm^2-sec. Obviously these levels are far in excess of the flux rates expected during flight.

Regarding heavy ions the rate of energy loss can be related to the rate of energy loss by protons by

$$\left.\frac{\partial E}{\partial x}\right|_{ion} = z^2 \left.\frac{\partial E}{\partial x}\right|_{proton}$$

where z is the charge state of the ion. One matter of little concern is the fact that z changes as the ion slows down. Obviously, the worst case occurs when the ion is fully ionized. Thus, for carbon, z = 12 or

$$\left.\frac{\partial E}{\partial x}\right|_{ion} = 144 \left.\frac{\partial E}{\partial x}\right|_{proton}$$

represents the worst case. Therefore, regarding ionization effects a flux of protons simulates a flux of fully ionized carbon ions at the same energy by reducing the proton flux rate by 144. Proton flux rates near 10^{12} protons/cm^2-sec at 576 MeV can be used to simulate approximately 10^{10} carbon ions/cm^2-sec at 576 MeV with the ions fully ionized. Clearly, this is far in excess of the expected heavy ion flux rates encountered in space.

A biref analysis of the experimental results will be given; however, there has been no significant attempt at a detailed model. Indeed, such a model would not add a great deal to the study. Regarding the decrease in firing voltage with ionization due to protons, there is no simple explanation of the observation. One expects the firing voltage to be relatively independent of residual ion-electron density for a dilute concentration. Basically avalanche breakdown depends upon the fact that the field must impart enough energy to the ionized electrons such that during their lifetime they can create one or more electron-ion pairs. Of course, there is the problem that in the total absence of electron-ion pairs, electrode phenomena must initiate avalance and consequently one may expect that irregularities in electrode geometry may cause unreliable firing. With ion-electron pairs available in the gas the avalanche process then becomes essentially a gas-dynamic process and the firing voltage should be relatively insensitive to the density of ion-electron ionized pairs. The observations indicate a dependence, however, a very small dependence since $V_f = \Phi^{-1/13}$.

Concerning the collection of ionized charge, the maximum voltage developed across the transducer is the order of a few volts even at the very high flux rates. Unfortunately, ionization outside the transducer

near the electrical connections could be responsible for most of the charge collected. However, the small voltage magnitude probably negates the need to give further consideration to the observations. A very simple analysis of charge collection within the transducer predicts about the voltage magnitude observed, however, the assumptions necessary to provide a tractable model make it difficult to be very definite regarding any conclusions about the origin of the voltage pulse.

Conclusions

From the experiments two conclusions appear reasonable. The simulation of ionizing radiation is far in excess of what is expected due either to protons or heavy ions. Secondly, the effects of the ionizing radiation upon the performance of the gas discharge transducer does not result in spurious signals which can be interpreted as impact events.

"Page missing from available version"

APPENDIX C

AMBIGUOUS SIGNAL GENERATION DUE TO HEAVY ION IRRADIATION

"Page missing from available version"

EXPERIMENTAL PROGRAM TO DETERMINE LONG-TERM CHARACTERISTICS OF THE MDE PRESSURE TRANSDUCERS

AMBIGUOUS SIGNAL GENERATION DUE TO HEAVY ION IRRADIATION

By L. K. Monteith

April 1972

Contract No. NAS1-10175
RTI No. 43U-568

Prepared for

National Aeronautics and Space Administration
Langley Research Center
Hampton, Virginia 23365

AMBIGUOUS SIGNAL GENERATION DUE TO HEAVY ION IRRADIATION

With respect to the discharge of an MOS capacitor type micrometeoroid detector along the track of a heavy ion, one can propose an analog which will allow qualitative arguments. Assuming the charge that is stored on the electrodes of the capacitor is to be transported through the ionization track of the heavy ion, the conductivity of the path will determine the magnitude of charge transported since the RC time constant for the discharge will be the resistance of the ionized media and the capacitance of the micrometeoroid capacitor-type detector. For a complete discharge of the capacitor one must assume that the RC time constant is short compared to the lifetime of the ionized media. The RC time constant T is given by

$$T = RC = \frac{\rho \ell}{a} \frac{\varepsilon A}{\ell} = \frac{\varepsilon A}{nq\mu a} = \frac{\varepsilon V}{Nq} \qquad (1)$$

where

$E \approx 0.33 \times 10^{-12}$ farads/cm

A = capacitor electrode area (~ 20 cm^2)

n = carrier density along the track of the heavy ion ($\approx 10^{20}$ along the track of a fission fragment in silicon)

N = total number of ionized carriers in volume $a\ell$,

q = electronic charge,

μ = mobility of carriers (Goodman estimates the electron mobility in SiO_2 to be ~30 cm^2/V-sec),

a = cross section of the ionization track of the heavy ion in cm^2,

R = resistance of the columnar ionization along the track of the heavy ion through SiO_2,

C = capacitance of the MOS capacitor,

ρ = resistivity of the ionized SiO_2,

ℓ = thickness of the SiO_2 (~10^{-4} cm), and

V = volume of SiO_2 (~ 2×10^{-3} cm^3).

Using the appropriate values results in

$$T \approx \frac{138}{N} \text{ seconds.} \qquad (2)$$

The appropriate value for N will depend upon the total energy lost by the heavy ion while traversing the SiO_2 film and the minimum energy necessary to ionize an electron in SiO_2.

For discharge through the ionization track to be effective the RC time must be small compared to the mean time (τ) the ionized electrons spend in the conduction state before immobilization into deep traps. Using a published value of $\mu\tau \approx 10^{-9} \frac{cm^2}{V}$ where $\mu \sim 30\ cm^2$,

$$\tau \approx 3 \times 10^{-11} \text{ seconds} . \tag{3}$$

For a full discharge to occur thru conduction $T < \tau \cong 3 \times 10^{-11}$ seconds. Thus,

$$N > 4.6 \times 10^{12} \text{ ionized carriers} . \tag{4}$$

A minor change is required to consider the case where $T \lesssim \tau$. The charge stored on the capacitor is reduced during discharge by

$$Q_C = Q_o\, e^{-t/T} . \tag{5}$$

Therefore during the time interval τ when conduction occurs

$$\frac{\Delta Q_C}{Q_C} = 1 - e^{-\tau/T} . \tag{6}$$

If $\tau < T$ the charge reduction on the capacitor is

$$\frac{\Delta Q}{Q_o} \approx 1 - \frac{\tau}{T} . \tag{7}$$

Therefore to achieve a 10% change in stored charge hence a voltage pulse that is 10% of bias voltage required $T \gtrsim 10\ \tau$. This results in $N \gtrsim 4.6 \times 10^{11}$ ionized carriers needed to provide conduction for the discharge during τ seconds.

Clearly the critical matter is the number of ionized carriers resulting from the passage of a heavy ion through the SiO_2. To estimate N we will consider the worst case. The maximum energy that a single heavy ion can give to an electron during the ionization event is

$$\Delta E = 4\, E_i \frac{m_e}{m_i} \frac{1}{1 + \left(\frac{m_e}{m_i}\right)^2} \tag{8}$$

where ΔE is the energy of the ionized electron, E_i is the energy of the heavy ion before the scattering event, m_e is the rest mass of the electron, and m_i is the rest mass of the heavy ion. That a single scattering event for the heavy ion is appropriate for the determination is obvious from considering the rate of energy loss per unit path length (dE/dx) and the thickness of the SiO_2. To simplify the analysis we will consider completely ionized heavy ions. In this case the dE/dx for heavy ions can be related to that of protons by

$$\left.\frac{dE}{dx}\right|_{ion} = z^2 \left.\frac{dE}{dx}\right|_{proton} \tag{9}$$

where z is the charge state of the heavy ion and assuming the velocity of the ion and the proton are the same and passage through the same absorber. For a completely ionized carbon ion with a kinetic energy near 1 BeV

$$\frac{dE}{dx} \quad 0.58 \frac{MeV}{cm} . \tag{10}$$

The thickness of the SiO_2 is the order of 10^{-4} cm, thus E $\simeq$ 58 eV. This indicates that the probability of multiple scattering of the incident heavy ion is very small indeed. Also, in the single scattering event the maximum energy is given by Equation 8.

Returning to a worst case analysis we will consider a single heavy ion scattering event producing a primary ionization electron with maximum kinetic energy of

$$E_{max} \approx 4 E_i \frac{m_e}{m_i} \tag{11}$$

where we have assumed $m_i >> m_e$. In addition we will assume that all the kinetic energy of the primary ionization electron is absorbed in secondary ionization producing N events requiring the minimum ionization energy per event. It has been shown that a reasonable estimate of the minimum ionization energy in a semiconductor is

$$E_o = \frac{3}{2} E_g \tag{12}$$

where E_o is the minimum ionization energy and E_g is the bandgap energy. For SiO_2, the minimum ionization energy as determined by Equation 12 is approximately 10 eV. Therefore, the total number of carriers produced in SiO_2 by a singly scattered heavy ion is

$$N \leq \frac{E_{max}}{E_o} = \frac{4 E_i}{10} \frac{m_e}{m_i} . \tag{13}$$

Returning to Equation 7 an estimate of the capacitor discharge due to 1 BeV fully ionized carbon in passi g through the MOS capacitor can be obtained as a worst case. For $\tau << T$ and int ducing Equations 2 and 3 into 7 yields

$$\frac{\Delta Q}{Q_o} = 1\text{-}2.2 \times 10^{-13} N . \tag{14}$$

For the 1 BeV carbon ion Equation 13 yields

$$N \leq 1.6 \times 10^4 \text{ ionized carriers} . \tag{15}$$

Therefore the discharge $\Delta Q/Q_o$ would be insignificant.

From this worst case analysis some attributes of the radiation induced conductivity as it relates to capacitor discharge are clearly identified. A single heavy ion which undergoes a single scattering event resulting in a cascade of secondary ionizations will not fully discharge the capacitor. The primary reason is the very short lifetime of the ionized carriers and the relatively small number of carriers created in a single event.

To be complete we should consider a steady state analysis for a flux of heavy ions. Again the key feature will be the carrier lifetime. However, the approach is slightly modified. The time constant for discharge is again

$$T = RC = \frac{\varepsilon}{nq\mu} \tag{16}$$

where in this steady state analysis the area for conductivity is assumed to be the full area A. This further assumes that the ion flux is uniformly distributed over this area. We must now evaluate n, the radiation induced carrier density in steady state or

$$\frac{\partial n}{\partial t} = g - \frac{n}{\tau} \tag{17}$$

where $\partial n/\partial t = 0$ in steady state, g is the ionized carrier density generation rate and τ the free carrier lifetime. Therefore, in steady state

$$n = g\tau \ . \tag{18}$$

We can obtain g from

$$g = \frac{\Phi}{E_o} \left.\frac{\partial E}{\partial x}\right|_{E_i} \tag{19}$$

where τ is the flux rate in ions per cm^2 per sec, E_o is the minimum energy necessary to ionize the carriers and $\left.\partial E/\partial x\right|_{E_i}$ is the average energy given up by the heavy ions of incident energy E_i in traversing x of SiO_2.

Using Equations 18 and 19 in Equation 16 yields

$$T = \frac{\varepsilon E_o}{\Phi \left.\frac{\partial E}{\partial x}\right|_{E_i} \mu\tau} = \frac{2 \times 10^{16}}{\Phi \left.\frac{\partial E}{\partial x}\right|_{E_i}} \tag{20}$$

where appropriate values for SiO_2 are used. For the 1 BeV fully ionized carbon ions $\partial E/\partial x\big|_{E_i} \simeq 0.58$ MeV/cm in SiO_2. To simplify matters consider $\partial E/\partial x\big|_{E_i} \simeq 1$ MeV/cm then Equation 20 becomes

$$T \simeq \frac{2 \times 10^{10}}{\Phi} . \tag{21}$$

The critical factor here is the recharge time constant for the capacitor. Assuming T is much longer than the recharge time constant, a low current drain on the power supply occurs, however, there is no transient discharge of the capacitor which could be counted as an impact. If T is much smaller than the recharge there would be transient voltages developed across the capacitor which could be counted. For the sake of analysis consider a 10% discharge then

$$\frac{Q_c}{Q_c} = 1 - e^{-\frac{t}{T}} = 0.1 . \tag{22}$$

or the time required to achieve this 10% charge for a given T is t = 0.1 T. If this t is much shorter than the recharge of the capacitor a 10% pulse could be counted. This could occur for

$$T = 0.1\ T = \frac{2 \times 10^{9}}{\Phi} . \tag{23}$$

For a given the time for a 10% discharge can be obtained. However, we know that the recharge time is less than 1 second. Therefore, for t to be less than 1 second, $\Phi < 10^9$ ions/cm^2-sec which is many orders of magnitude above the expected heavy ion flux rate. Therefore, the steady state analysis also indicates that discharge pulses are unlikely due to a flux of heavy ions.